

**UNCLASSIFIED**

---

**AD 276 397**

*Reproduced  
by the*

**ARMED SERVICES TECHNICAL INFORMATION AGENCY  
ARLINGTON HALL STATION  
ARLINGTON 12, VIRGINIA**



---

**UNCLASSIFIED**

NOTICE: When government or other drawings, specifications or other data are used for any purpose other than in connection with a definitely related government procurement operation, the U. S. Government thereby incurs no responsibility, nor any obligation whatsoever; and the fact that the Government may have formulated, furnished, or in any way supplied the said drawings, specifications, or other data is not to be regarded by implication or otherwise as in any manner licensing the holder or any other person or corporation, or conveying any rights or permission to manufacture, use or sell any patented invention that may in any way be related thereto.

TECHNICAL OPERATIONS INCORPORATED

276 397

276 397

MODELING TECHNIQUES AS APPLIED  
TO FALLOUT SIMULATION ON RESIDENTIAL-TYPE  
STRUCTURES AND SOME PRELIMINARY RESULTS

By

Albert W. Starbird  
John F. Batter, Jr.  
Herbert A. Mehlhorn

8 July 1961  
TO-B 61-35

Prepared for

Office of Civil Defense and Mobilization  
Contract CDM-SR-60-45

tech ops

tech ops

**TECHNICAL OPERATIONS**

**incorporated**

**MODELING TECHNIQUES AS APPLIED  
TO FALLOUT SIMULATION ON RESIDENTIAL-TYPE  
STRUCTURES AND SOME PRELIMINARY RESULTS**

By

Albert W. Starbird  
John E. Batter, Jr.  
Herbert A. Mehlhorn

8 July 1961  
TO-B 61-35

Prepared for

Office of Civil Defense and Mobilization  
Contract CDM-SR-60-45

**Burlington, Massachusetts**

## ACKNOWLEDGMENTS

The authors wish to thank the many individuals who helped to make this project possible. The following deserve particular attention:

Dr. Eric T. Clarke, who helped to organize and guide the project

Mr. Arthur Kaplan and Dr. Raymond Gold, for their technical analysis and valued advice

Mr. Robert R. McMath, who worked long hours on the actual performance of the experimentations.



## ABSTRACT

In this project, an experimental study of the radiation attenuation of two residential-type structures was made. The two model structures investigated were surrounded with rings and annular areas of simulated fallout by pumping a 10-curie, cobalt-60 source through plastic tubing at a constant velocity. Radiation measurements were taken with time-integrating detectors.

This report describes the theory of measuring radiation effects with models and the facility developed for OCDM at Technical Operations, Incorporated, Burlington, Massachusetts, to conduct these experiments. It concludes with a comparison of experimental data obtained in these tests with data obtained in previous full-scale tests made on identical structures at the Nevada Test Site.

## TABLE OF CONTENTS

<u>Chapter</u>		<u>Page</u>
1	INTRODUCTION .....	1
2	MODELS AND SCALING .....	3
3	SCALE MODEL FACILITY AND EQUIPMENT .....	6
	SCALE MODEL FACILITY .....	6
	EXPERIMENTAL EQUIPMENT .....	8
	INSTRUMENTATION AND DOSIMETER CALIBRATION ...	12
4	EXPERIMENTAL MEASUREMENTS .....	18
	INTRODUCTION .....	18
	MODEL EXPERIMENTS FOR THE PRECAST CONCRETE HOUSE .....	18
	1. Description of Full-Scale and Model Structures ...	18
	2. Experimental Procedures .....	22
	3. Measurements and Results .....	24
	4. Discussion of Model Results .....	33
	TWO-STORY, WOODEN-FRAME HOUSE AREA SPREAD EXPERIMENTS .....	46
	1. Description of the Two-Story House .....	46
	2. Experimental Procedures .....	54
	3. Measurements and Results .....	56
	4. Discussion of Model Results .....	60
	4.1 Upper Floors of Two-Story House .....	63
	4.2 Basement of Two-Story House .....	67
5	SUMMARY.....	73

TABLE OF CONTENTS  
(Continued)

<u>Appendixes</u>	<u>Page</u>
A      NORMALIZATION OF MODEL DATA .....	A-1
Precast Concrete House Source Ring Normalization ....	A-1
Two-Story House Area Simulation .....	A-3
B      TRANSPARENT-BUILDING CALCULATIONS .....	B-1
Present Concrete House With Source Rings .....	B-1
Two-Story Model Building With Area Spread .....	B-3
C      DOSE RATES FROM ANNULAR SOURCE FIELDS .....	C-1
Validity of Approximate Formulation Using a Mean	
Source-to-Detector Distance .....	C-1
Evaluation of Dose Rates for an Infinite Field from the	
Approximation Formulation .....	C-5



# LIST OF ILLUSTRATIONS

<u>Figure</u>		<u>Page</u>
1	Plan View of Model Facility . . . . .	7
2	Photographic View of Model Facility . . . . .	8
3	Diagram of Source Circulation System . . . . .	10
4	Photograph of 10 Curie Co-60 Source Container . . . . .	11
5	Calibration of 10-Milliroentgen Dosimeter . . . . .	14
6	Calibration of 200-Milliroentgen Dosimeter . . . . .	15
7	Calibration of 2-Roentgen Dosimeter . . . . .	16
8	Photograph of Scale Model of Precast Concrete Ranch House . . . .	19
9	Photograph of Full-Size Precast Concrete Ranch House . . . . .	20
10	Model Precast Ranch House Showing Dosimeter Placement . . . . .	21
11	Floor Plan and Dosimeter Locations for the Precast Concrete Model Ranch House . . . . .	26
12	Precast Concrete House, Horizontal Traverse along Hallway 3 Inches above Floor; 42.5-Inch Source Radius . . . . .	37
13	Precast Concrete House, Horizontal Traverse along Centerline of Living Room 3 Inches above Floor; 42.5-Inch Source Radius . . . .	37
14	Precast Concrete House, Horizontal Traverse along Centerline of Living Room 7 Inches above Floor; 42.5-Inch Source Radius . . . .	38
15	Precast Concrete House, Horizontal Traverse along Rear Wall of Master Bedroom 3 Inches above Floor; 42.5-Inch Source Radius .	38
16	Precast Concrete House, Horizontal Traverse along Hallway 3 Inches above Floor; 42.5-Inch Source Radius . . . . .	39
17	Precast Concrete House, Horizontal Traverse along Living Room 3 Inches above Floor; 42.5-Inch Source Radius . . . . .	39
18	Precast Concrete House, Horizontal Traverse along Living Room 7 Inches above Floor; 42.5-Inch Source Radius . . . . .	40
19	Precast Concrete House, Horizontal Traverse from Back to Front of Living Room 3 Inches above Floor; 42.5-Inch Source Radius . .	40
20	Precast Concrete House, Horizontal Traverse along Rear Wall of Master Bedroom 5 Inches above Floor; 25.5-Inch Source Radius. .	41
21	Precast Concrete House, Horizontal Traverse along Hallway 3 Inches above Floor; 25.5-Inch Source Radius. . . . .	41

LIST OF ILLUSTRATIONS  
(Continued)

<u>Figure</u>	<u>Page</u>
22 Precast Concrete House, Horizontal Traverse from Back to Front of Living Room 3 Inches above Floor; 25.5-Inch Source Radius . .	42
23 Precast Concrete House, Horizontal Traverse along Centerline of Living Room 3 Inches above Floor; 25.5-Inch Source Radius . . . .	42
24 Precast Concrete House, Horizontal Traverse along Centerline of Living Room 5 Inches above Floor; 25.5-Inch Source Radius . . . .	43
25 Precast Concrete House, Horizontal Traverse along Centerline of Living Room 7 Inches above Floor; 25.5-Inch Source Radius . . . .	43
26 Photograph of Full-Size, Two-Story, Wooden-Frame House . . . .	47
27 Photograph of Scale Model of Two-Story, Wooden-Frame House . .	47
28 Two-Story Model House Showing Placement of Dosimeters . . . . .	48
29 Plan View of First Floor Giving All Dosimeter Locations for . . . . Two-Story House . . . . .	50
30 Plan View Giving Dosimeter Positions for the Second Floor of Two-Story Model House . . . . .	51
31 Plan View Giving Dosimeter Positions for the Basement of Two-Story Model House . . . . .	52
32 Typical Vertical Section of Two-Story Model House . . . . .	53
33 Vertical Plot of Protection Factors at Center of Two-Story Model House . . . . .	64
34 Vertical Plot of Protection Factors at Center of Living Room in Two-Story Model House . . . . .	64
35 Protection Factors for First Floor of Two-Story Model House . . .	65
36 Protection Factors for Second Floor of Two-Story Model House . .	66
B-1 Dose Rate for Transparent House in Center of 25.5 Foot-Radius Source Ring . . . . .	B-2
B-2 Dose Rate for Transparent House in Center of 42.5 Foot-Radius Source Ring . . . . .	B-2
B-3 Dose Rate Versus Dosimeter Height for Transparent Model House in Center of Annular Source Areas . . . . .	B-5

# LIST OF TABLES

<u>Table</u>		<u>Page</u>
I	Dosimeter Calibration Conditions . . . . .	13
II	Experiments Performed on the Model Precast Concrete Ranch House . . . . .	25
III	Dose Rate Data for Precast Concrete House (42.5 Foot-Radius Source Ring Simulated) . . . . .	27/28
IV	Dose Rate Data for Precast Concrete House (42.5 Foot-Radius Source Ring Simulated, Living Room Door and Window Blocked with 3-1/2 Inch-Thick Cement) . . . . .	31/32
V	Dose Rate Data for Precast Concrete House (25.5 Foot-Radius Source Ring Simulated) . . . . .	34/35
VI	Dose Rate Data for Two-Story Model House . . . . .	59
VII	Dose Rate Data for Basement of Two-Story Model House . . . . .	60
VIII	Two-Story Model House Protection Factors Compared to Full-Scale House of Same Wall Thicknesses. . . . .	62
IX	Dose Rates of Basement in Two-Story, Wooden-Frame House . . . . .	68
X	Ratio of Scattered Dose in the Basement of Two-Story, Wooden-Frame House to Direct Dose above Infinite Plane . . . . .	69
XI	Comparison of Dose Rate in Basement of Two-Story, Wooden-Frame House to that of Two-Story Model House . . . . .	71
I-C	Comparison of Taylor Expansions of True Dose Function, $A(\eta)$ , for $P = 106.07$ Feet, $\mu = 448$ Feet . . . . .	C-4

(7)

## CHAPTER 1

### INTRODUCTION

The theory of radiation protection in complex structures is one that has received considerable attention during the last few years. In principle, the radiation protection offered by a structure is a simple function of the geometry and mass shielding of the structure. Complications arise, however, when consideration is given to real structures which have non-uniform wall thicknesses, apertures, and complicated geometries.

Considerable effort has been expended in the simplification of the computation procedures needed to predict the attenuation provided by a real structure. Most simplifying procedures have led to assumptions regarding the effects of local discontinuities in the structure. In order that these simplifications, and consequently assumptions, may be properly evaluated, a program of experimental measurements of real structures was instituted by the Office of Civil Defense and Mobilization in the summer of 1957. The principal difficulties in carrying out tests on real structures are compounded by: 1) a general lack of structures of interest secluded enough to establish adequate radiation-exclusion areas, 2) the enormous costs involved in carrying out field experiments, and 3) the lack of controllability of extraneous influences, such as inclement weather, on the personnel and equipment involved.

To overcome these difficulties, consideration was given to building inexpensive, small-scale models of the structures, which would still be adaptable to the proposed experimentation. Preliminary experiments on the utility of the modeling approach were first performed in the fall of 1958.<sup>1</sup> These experiments, performed on a modest scale, confirmed that the modeling approach to the measurement of radiation attenuation in structures could be quite useful, and was both an economical and convenient solution to the problem.

---

<sup>1</sup>Eric T. Clarke, John F. Batter, Jr., and Arthur L. Kaplan, "Measurement of Attenuation in Existing Structures of Radiation from Simulated Fallout," Technical Operations, Incorporated, Report No. TO-B 59-4, 27 April 1959.

Chapter 2 describes the substitution of models for full-scale structures in radiation-attenuation measurements by alluding to three basic guides used in model construction. These guides predicate that the densities of all materials used in the model technique, including building materials, the ground, and the surrounding atmosphere, should be increased by the same scaling factor that governs reduction of the structure's linear dimensions.

Chapter 3 describes the scale model facility and equipment used in the measurements, with brief mention of the instrumentation and dosimeter calibration techniques.

In Chapter 4, the experimental measurements on both the precast concrete model house and the two-story, wooden-frame model house are discussed in detail. The chapter includes descriptions of each of the houses, the experimental procedures used, measurements and results, and a discussion of the results for each of the two models.

Chapter 5 presents a summary of conclusions based on the measurements conducted.

The report concludes with three appendices, which provide the analytical procedures for reduction of the experimental data.

## CHAPTER 2

### MODELS AND SCALING

In theory, the radiation-dose distribution inside a structure, due to activity distributed outside, will be exactly reproduced in a scale model, if all materials, including the surrounding ground and atmosphere, as well as those comprising the structure, are increased in density by the same scale factor, but are otherwise unchanged. Perfect scaling may be achieved if the following three basic laws are obeyed in the construction of the model:

1. All dimensions must be linearly scaled by the same factor
2. Each absorbing surface must attenuate radiation to the same degree as the original surface, independent of the linear scaling factor
3. The specific scattering and absorption properties (such as cross sections and mass-attenuation coefficients) of all materials must remain unchanged.

These rules lead to the conclusion that the densities of all materials, including the building materials, the ground, and surrounding atmosphere, should be increased by the same scaling factor that reduces linear dimensions. That is, the product of density times thickness is unchanged for each material. In practice, the problem of increasing densities by a factor large enough to be useful in reducing building dimensions makes it difficult to achieve this ideal. Scaling must be by a factor of 10 to provide much advantage over working with the original full-size structure. It is necessary, therefore, to find methods approximating these requirements.

Most of the technique of modeling depends on determining what requirements can be safely relaxed. As a first approximation, iron was substituted for concrete and other building materials to increase the density as much as possible without changing the atomic number of the material too greatly. This permitted an increase in average density of approximately 3. Secondly, it was believed that scaling would still be realistic, if the wall thicknesses were not permitted to be more than 10 per cent of the average dimensions of any given room. This criterion permitted the walls to be increased in total mass by another factor of 3 or 4. As a result, we

○

were able to achieve a factor of 12:1 on the scaling dimensions. In one of the models which will be described, the original wall thickness was made of 6 inches of light-weight concrete, while the scale model was constructed of 1-inch iron plate. No attempt was made to scale the densities of either the atmosphere or the ground surrounding the building. As a result, skyshine was not properly reproduced in the modeling. However, many buildings of interest are thick enough, so that the largest contribution to the radiation within the building is produced either by gamma rays directly from the source outside or from rays scattered by the walls and ceilings of the building itself.

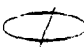
Simulation of the skyshine effect could be approximated if the model and source configuration were roofed over to an approximate mean-free-path with a material approximating the scattering properties of the atmosphere. This is a fairly expensive and complicated proposition as the weights of material required are large, and hence physical difficulties are introduced in the set-up and performance of an experiment. The results described in Chapters 3 and 4 of this report have been obtained neglecting skyshine simulation. Because of this, they may be low by a maximum of about 10 per cent.

Since an accurate reproduction of the relative scattering and absorption of the materials at all basic wavelengths must be approximated, there is some ambiguity in selecting the criteria for computing model wall thicknesses. Three points of comparison with full-scale walls can be made:

1. Mass thickness may be matched
2. Broad-beam absorption data for flat slabs can be applied
3. Electron density may be maintained.

To illustrate this, we observe that 6 inches of light-weight concrete is equivalent to 1.20 inches of iron on the basis of mass thickness. The same broad-beam attenuation will be produced by 1.19 inches of iron. However, maintaining constant electron density in the iron and concrete walls leads to a value of 1.02 inches of iron, somewhat lower than that obtained by the first two criteria.

One problem introduced by the use of iron as a substitute for more common building materials is that iron effectively removes much of the lower-energy gamma



rays. Thus, if a model were constructed on the basis of broad-beam attenuation coefficients, and comparisons to an actual structure were made, there would be a heavy dependence on the linearity of the detector with gamma-ray energy. An approach to the solution of this problem would be to construct model walls with laminates of masonite and iron, not only to reproduce the broad-beam attenuation, but also to approximate the energy spectrum.



## CHAPTER 3

### SCALE MODEL FACILITY AND EQUIPMENT

#### SCALE MODEL FACILITY

A facility for conducting gamma-ray experiments on model buildings was constructed during the spring of 1960 on Technical Operations' 6-acre site in Burlington, Massachusetts. This site was adjacent to the firm's main office building, permitting easy access to the radiographic facilities, shops, and personnel. Figure 1 gives a plan view of the model facility, and Figure 2 shows the facility with two model houses surrounded by the polyethylene tubing which carries the radioactive source.

A six-foot high outer personnel protection fence with two normally locked service gates and one personnel entrance gate (with alarm) was constructed around the site. "Caution, Radiation Area" signs were posted on this fence at 50-foot intervals. A 100- by 100-foot flat test pad with asphalt surface was constructed near the center of the enclosed area. Two concrete foundations 4-1/2 by 6 by 2 feet deep were recessed flush in the pad to permit testing of model buildings with basements. One foundation was located at the center of the pad, permitting 360-degree area spread and source ring experiments, and the other was positioned near one corner of the pad for quarter-symmetry experiments. An inner fence was erected at a minimum distance of forty feet from the edge of the pad to serve as a high-radiation (100 mr/hr) area boundary. "Caution, High-Radiation Area" signs were attached to this fence at 50-foot intervals. Chain gates were provided for the two entrances to the test pad. A 25-foot high pole was erected at each corner of the pad for flood lighting and to allow stringing of cables over the pad. An earth mound 12-feet high was formed on the east side of the pad from boulders and other fill material removed during rough grading of the pad. Behind the mound, a 16 by 20-foot control and storage building was erected. The mound provided excellent protection to operating personnel during radiation experiments. The small combined control and storage building, plus a narrow paved path connecting with the pad, were constructed at pad level to permit wheeling of heavy lead source containers from the storage area to the test pad.



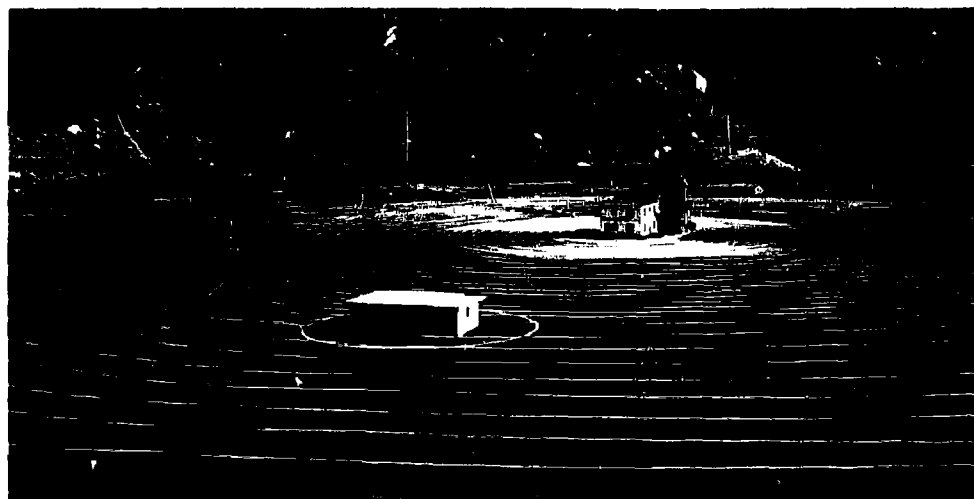


Figure 2. Photographic View of Model Facility

This scale model facility proved very convenient for conducting model experiments. Radiation levels at the outer fence during exposures with a 10-curie, cobalt-60 source were 0.5 mr/hr (milliroentgens per hour) or less as compared to an AEC-allowable limit of 2.0 mr/hr. During radiation experiments, the long slope on the south side of the facility permitted direct observation of activities on the entire test pad, plus 90 per cent of the area enclosed by the outer fence. From a vantage point 200 feet up this slope, the motion of the source through the lengths of polyethylene tubing was checked and measured with a 20-power spotting scope.

#### EXPERIMENTAL EQUIPMENT

The equipment required for pumping an encapsuled source through rings or area spreads of polyethylene tubing is similar to that previously developed and used by Technical Operations, Inc., for full-scale building tests. This type of equipment was described in detail in previous reports,<sup>2,3</sup> and will not therefore be covered in as much detail in this report.

<sup>2</sup>Clarke, Batter, and Kaplan, op. cit.

<sup>3</sup>J. F. Batter, et al., "An Experimental Evaluation of Radiation Protection Afforded by a Large Modern Concrete Office Building," Technical Operations, Inc., Report No. TO-B 59-5, May (1959) and CEX 59.1 AEC, May (1959).

(1)

A schematic of the hydraulic system for source circulation is shown in Figure 3. Water from the reservoir is drawn into the appropriate pump or pumps and then forced through the source container in a manner calculated to drive the source out of the container and through the polyethylene tubing. A gear pump and the feeds of two metering pumps were connected in parallel and valved for independent operation as well as for any combination of the three. The gear pump was used for filling the system quickly and for rapid movement of the source when a metered flow (for accuracy) was not required. A Hills-McCanna two-feed metering pump was used for accurate flow control between 0.36 and 13.6 gph. For maximum versatility, one feed of the pump had a capacity of 3.6 gph and the other 10.0 gph. Output of these pumps could be rapidly changed through use of a micrometer adjustment of the pump stroke. A pressure gage was used for visual monitoring of system pressure and a relief valve was used for protection of the hydraulic system. Flow from the pumps passed into a 3-way solenoid valve wired for remote operation. This valve allowed either bypassing the pump output directly to the reservoir or diverting the flow to the source storage container, and thence into the ring or area spread tubing.

The source container (shown in Figure 4) consisted of a 1000 pound, lead-filled steel shell mounted on wheels. Two stainless-steel tubes of the same internal diameter as the polyethylene tubing passed lengthwise through the center of the container. These tubes contained a horizontal radius bend to eliminate direct streaming of gamma-rays from the source container. The source was pumped from the container tube (where it was stored) through the ring or area spread, and then returned to the second tube of the storage container. Special fittings which allowed the tubing to be easily detached from, or re-attached to, the storage container were developed. These fittings were made of stainless steel, were self-aligning to prevent sticking of the source at the joint, and were leak-tight at a 2000 psi proof test pressure (actual operating pressure, however, did not exceed 150 psi). The fittings could be screwed together finger-tight with perfect performance assured. Thus, the connections could be easily changed without tools. Neoprene O-ring seals were used as seals at the fittings. A fitting was installed on the polyethylene tube returning from the container to the water reservoir to stop positively the source at the center of the container and prevent it from continuing through the container to the reservoir.

**Figure 3. Diagram of Source Circulation System**



Figure 4. Photograph of 10 Curie Co-60 Source Container

In addition, two clamp fittings were attached to the source container tubes, one to lock or clamp the source in a safe position within the container just before its use, and the second, used in conjunction with the stop fitting, to clamp the source in a proper safe position on its return to the container. During tests, the stop fittings remained with the container and were on diametrically opposite ends. The two remaining source-container fittings were painted red for safety and were connected to a pressure hose from the pumps and to the return end of the area spreads, depending on orientation of the source in the container. A padlock-safety plug arrangement was provided for locking the source in the center of the container when it was not in use. The cobalt-60 source material was contained within a 3/16-inch diameter by 1 3/4-inch long capsule, triple-sealed for leak-tightness. A short, flexible length of stainless steel connected the capsule to a piston consisting of a stainless plug with a pump leather-type water seal. Water pressure behind the piston forced it and the attached source capsule through the tubing.



was exposed to a 45-millicurie source of cobalt-60 for 35 minutes with all dosimeters 18.5 cm from the source. Scattering within the laboratory, which should have been the same for all dosimeters, provided a small part of the exposure. Most of the dosimeters were about 50 per cent discharged as expected. A few produced readings markedly different (30 to 60 per cent) from the others. These were withdrawn from use. For one of these exposures, the average reading for 58 dosimeters was 52.1  $\mu$ a. The root mean square deviation was 3.02  $\mu$ a or  $\pm 5.8$  per cent when referred to the 52.1  $\mu$ a average. Repetition of this procedure several times during the experimental work produced essentially the same statistical results. On a nonstatistical basis, some dosimeters which read above the average in one exposure of 60 dosimeters might read below in the next exposure. This was mentioned earlier.

The calibration of dosimeters necessary to convert  $\mu$ a readings from the charger-reader to dose values in mr was conducted outdoors to reduce scattering into the dosimeters. Care was taken to place the dosimeters at heights above the ground that would minimize local effects of ground scattering without unduly complicating the procedure. All exposures were to cobalt-60 sources of known strength. In each case, groups of identical dosimeters were placed a given distance from the source. Different exposures were obtained by varying the time of exposure. The dose was calculated based on an inverse square law behavior for source-to-dosimeter distance and no scattering. Table I summarizes the experimental conditions and presents conversion factors to obtain dose in mr from charger-reader data in  $\mu$ a.

TABLE I  
DOSIMETER CALIBRATION CONDITIONS

Dosimeter	Source Strength (curie-Co-60)	Source Height (meters)	Dosimeter Height (meters)	Source-to- Dosimeter Distance (meters)	Dose Rate (r/hr)	Conversion Ratio (mr/ $\mu$ a)
10 mr	9.6	0.00	7.35	12.00	0.090	0.112
200 mr	2.1	4.00	4.00	4.00	0.179	2.3
2r	2.1	0.80	0.80	1.19	2.000	*

\* Below 25  $\mu$ a, 16 mr/ $\mu$ a; above 25  $\mu$ a, 21.4 mr/ $\mu$ a minus 150 mr; see text.



For the 10-mr. dosimeters, a single group of five was given successive exposures of increasing duration. The average characteristics are plotted in Figure 5. Variations among dosimeters which were identically exposed fell within about  $\pm 3$  per cent of the average figures, across the entire dosage range.

The 200-mr dosimeters were divided into two groups of three, which were alternately given exposures of increasing duration. Variations among identically exposed dosimeters were minor. Average characteristics are plotted in Figure 6.

The 2r dosimeters were stacked three high in twenty groups, all equidistant from the source. Groups of three were successively withdrawn at fixed intervals of time which represented 100-mr increments of dose. The average characteristics are plotted in Figure 7 with points shown for individual dosimeters. The vertical spread of points for dosimeters receiving the same exposure falls within  $\pm 3$  to 4  $\mu$ a

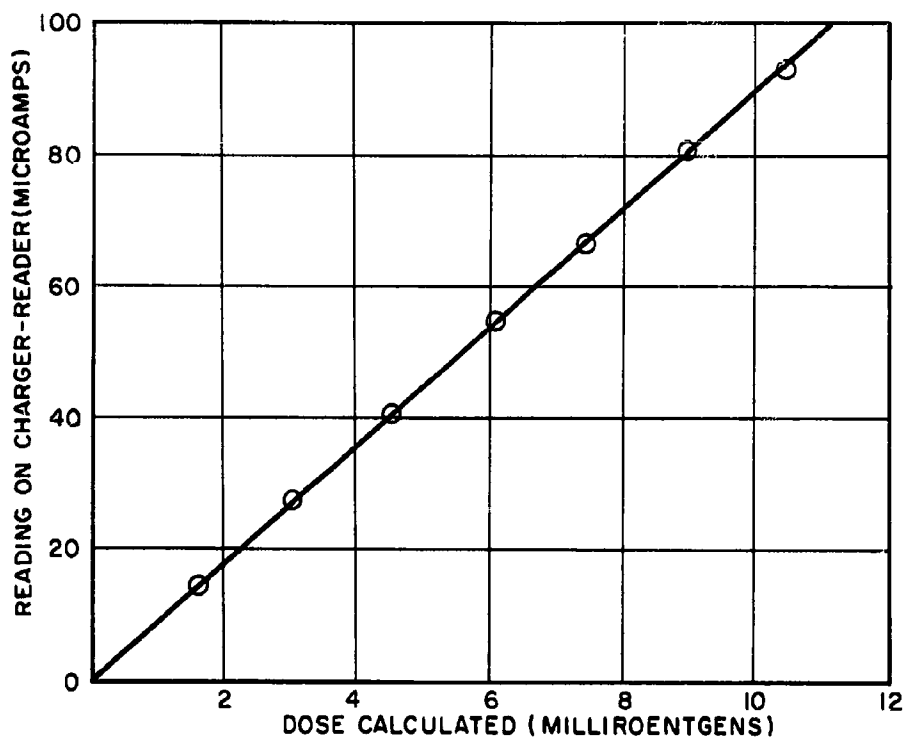


Figure 5. Calibration of 10-Milliroentgen Dosimeter

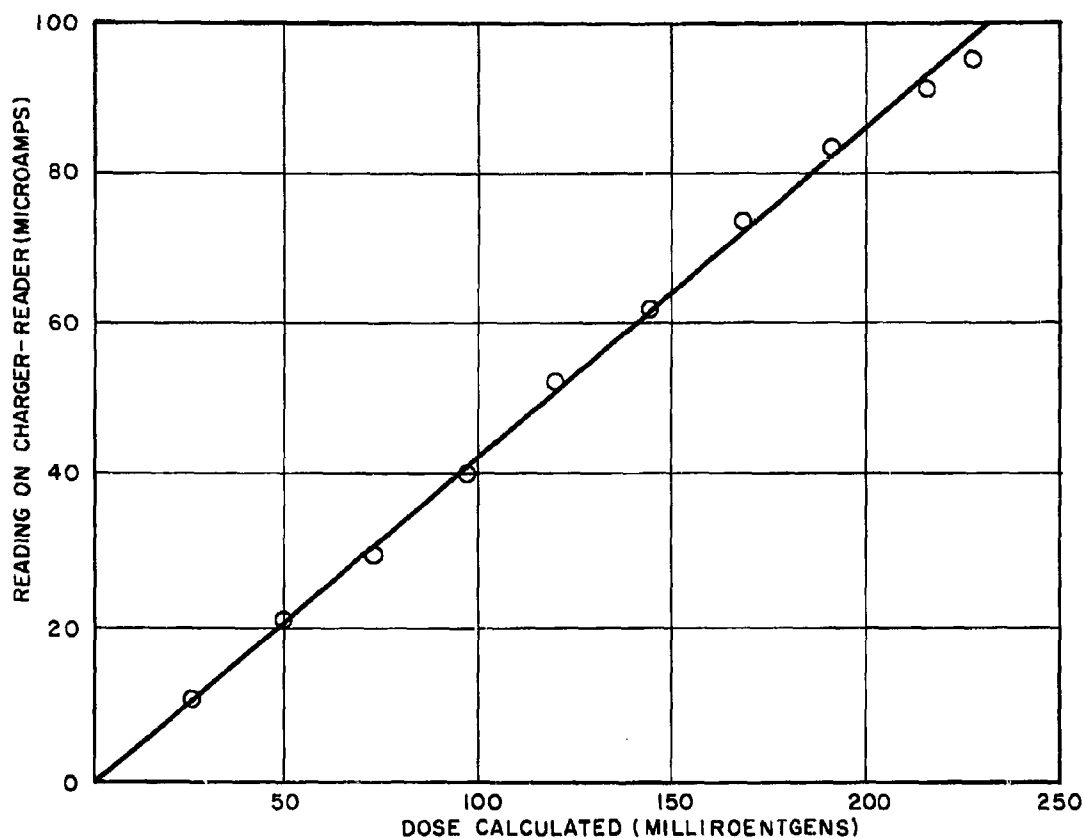


Figure 6. Calibration of 200-Milliroentgen Dosimeter

across the exposure range. Unlike the figures for the 10-mr and 200-mr dosimeters, the 2r dosimeters are not linear. The curve of Figure 7 can be represented by two linear sections intersecting at  $27.8 \mu\text{a}$ . The first section passes through  $(0, 0)$  with a slope of  $1/16 \mu\text{a}/\text{mr}$ . The second has an intercept at  $7.0 \mu\text{a}$  and a slope of  $1/21.4 \mu\text{a}/\text{mr}$ . The bend in the characteristic curve is a consequence of the dosimeters' construction. Whereas some dosimeters are a single coaxial capacitor, this one has a center conductor made in two sections which are not in contact except during the charging and reading of the dosimeter. The short section is a pin centered in a flexible diaphragm at one end of the dosimeter. When the dosimeter is pressed into the socket on the charger-reader, the diaphragm flexes so that the pin contacts the

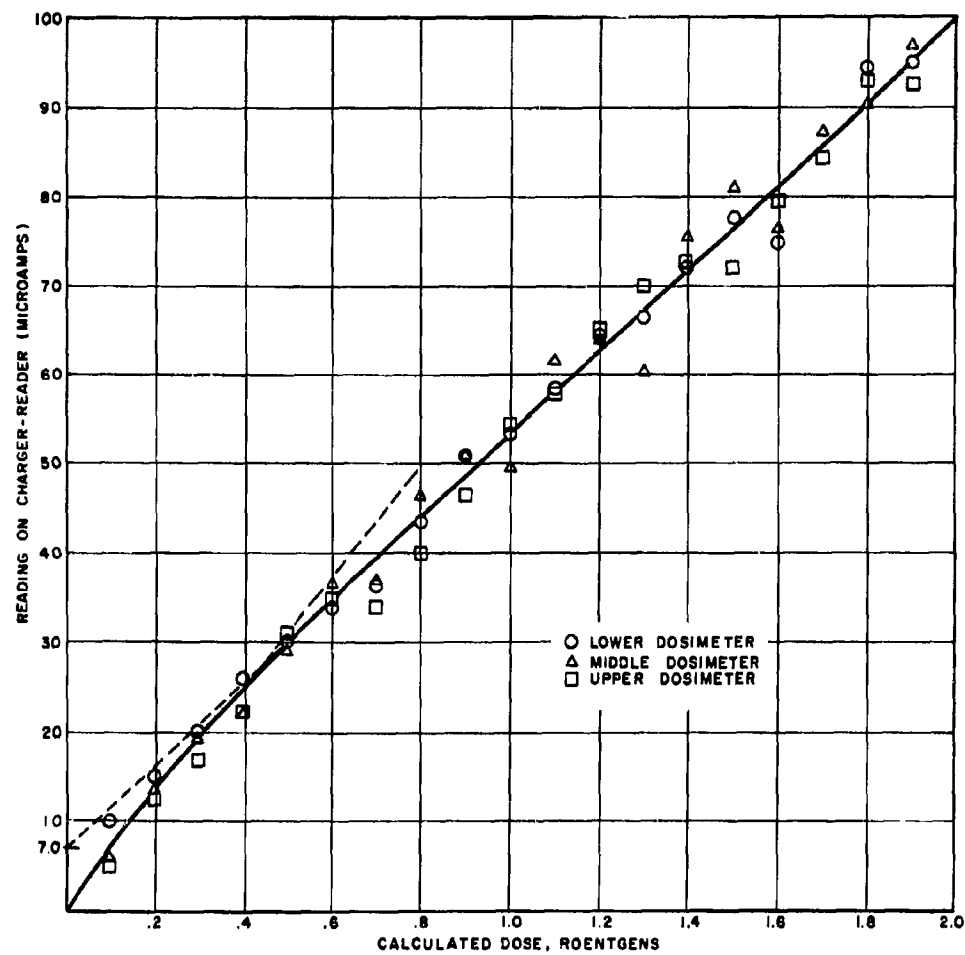


Figure 7. Calibration of 2-Roentgen Dosimeter

(1)

center conductor in the main body of the dosimeter. Both the pin and the center conductor are charged. Upon withdrawal of the dosimeter after charging, the pin loses contact with the center conductor. There are then two dosimeters in the same shell. During exposure to radiation both are discharged with the larger volume dosimeter in the main body losing more charge. Apparently the pin is completely discharged at the start of the linear characteristic at 445 mr and  $27.8 \mu\text{a}$  on Figure 7. If both sections of the dosimeter had the same capacity per unit length and the same active volume per unit length, they would lose equal fractions of their original charge during exposure and eventually reach a full-scale condition together ( $100 \mu\text{a}$  reading on the charger-reader). It is possible to establish a theoretical calibration curve for the two dosimeters which are exposed and read as one, from knowledge of the capacity of the individual sections and the active volumes for each in which ionization occurs under exposure. Accurate measurements of the volume are difficult and were not undertaken. However, the readings of the charger-reader, in  $\mu\text{a}$ , are directly proportional to the amount of charge neutralized by radiation. Repeated readings have shown that when the pin is not in contact with the remainder of the dosimeter, a fully discharged pin produces a  $7\text{-}\mu\text{a}$  reading while  $100 \mu\text{a}$  is obtained for a full-scale dosimeter reading when the pin makes contact. This is consistent with the  $7\text{-}\mu\text{a}$  intercept obtained by extrapolation of the linear portion of Figure 7. The curve in that figure may be represented by:

$$\begin{aligned} \left(16.0 \frac{\text{mr}}{\mu\text{a}}\right) y &= x & 0 < x < 445 \text{ mr} \\ \left(21.4 \frac{\text{mr}}{\mu\text{a}}\right) (y - 7.0) &= x & 445 < x < 2000 \text{ mr} \end{aligned}$$

where  $y$  is in  $\mu\text{a}$  and  $x$  in mr.

The linear functions just given were used for interpreting data obtained with the 2r dosimeters but the discontinuity in the conversion from  $\mu\text{a}$  to mr was made at the point (400 mr,  $25 \mu\text{a}$ ) as a matter of convenience.

## CHAPTER 4

### EXPERIMENTAL MEASUREMENTS

#### INTRODUCTION

Experimental dose measurements were made for two 1/12-scale buildings to obtain a comparison between modeling techniques and full-scale measurements, and to gather original data using model buildings. The buildings were a steel model of a precast, concrete house, and a steel model of a two-story, wooden-frame house. Radiation was from cobalt-60 in all cases.

Experiments with the precast concrete model building were performed to develop and refine modeling techniques by comparing modeling results with similar full-scale experimental results.<sup>4</sup> Individual source rings of 25.5- and 42.5-inch radii were used. For the larger ring, data was taken with the living room door and windows blocked and unblocked. These measurements modeled the full scale work with source rings of 25.5- and 42.5-foot radii.

Additional measurements were made of the radiation protection afforded by a typical two-story house. These experiments were performed using an area source to simulate contamination on the ground out to a radius of 45 feet from the center of the model. The results of this experiment provided new and original data on the radiation protection that would be provided by a common type of two-story house with light wall construction.

#### MODEL EXPERIMENTS FOR THE PRECAST CONCRETE HOUSE

##### 1. Description of Full-Scale and Model Structures

The first scaled building, a 1/12-model of the precast concrete house at the Nevada Test Site, was constructed of steel and evaluated for the attenuation of gamma-rays from source rings. Source rings for the experiments were simulated by pump-

---

<sup>4</sup>J. A. Auxier, J. O. Buchanan, C. Eisenhauer, and H. E. Menker, "Experimental Evaluation of the Radiation Protection Afforded by Residential Structures against Distributed Sources," CEX-58, 1, AEC, 19 January (1959).

ing a cobalt-60 source at a uniform rate through rings of polyethylene tubing.

The full-scale concrete house<sup>5</sup> was a single-story building constructed on a 4 inch-thick concrete floor slab. The outside dimensions of the building were 40 feet long by 27-1/2 feet wide, exclusive of 2-foot roof overhang. The floor-to-ceiling height was 8 feet. All walls, partitions, and roof panels were of 6 inch-thick pre-cast lightweight (98 lb/ft<sup>3</sup>) expanded shale-aggregate concrete. The floor slab finish surface for the house was approximately 1 foot above grade and 8 inches above the attached garage floor.

A photograph of the steel model of this building, surrounded by tubing for the source ring appears as Figure 8. Figure 9 is a photograph of the full-scale structure. Figure 10 shows the partition arrangement through an open roof. The external

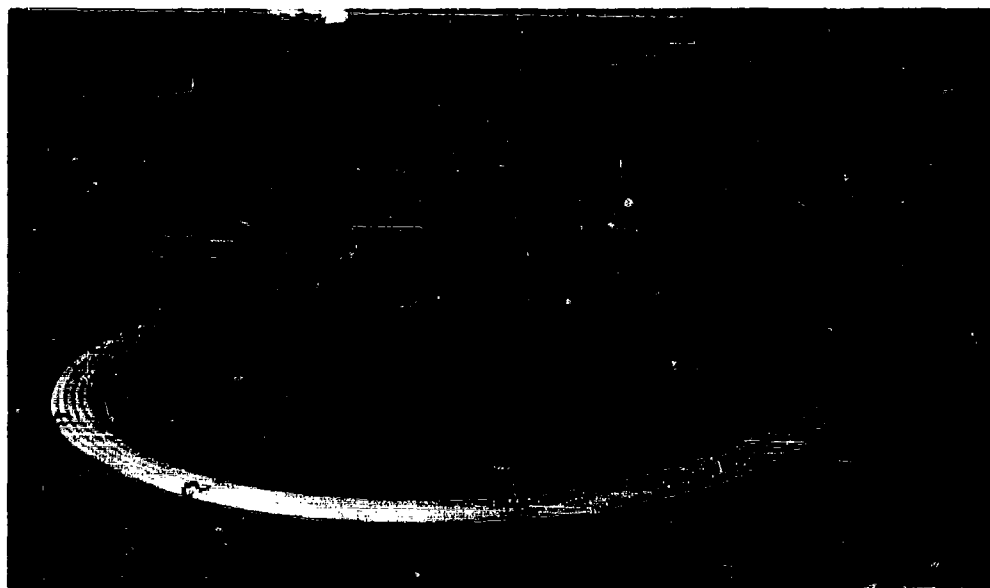


Figure 8. Photograph of Scale Model of Precast Concrete Ranch House

---

<sup>5</sup>Ibid.

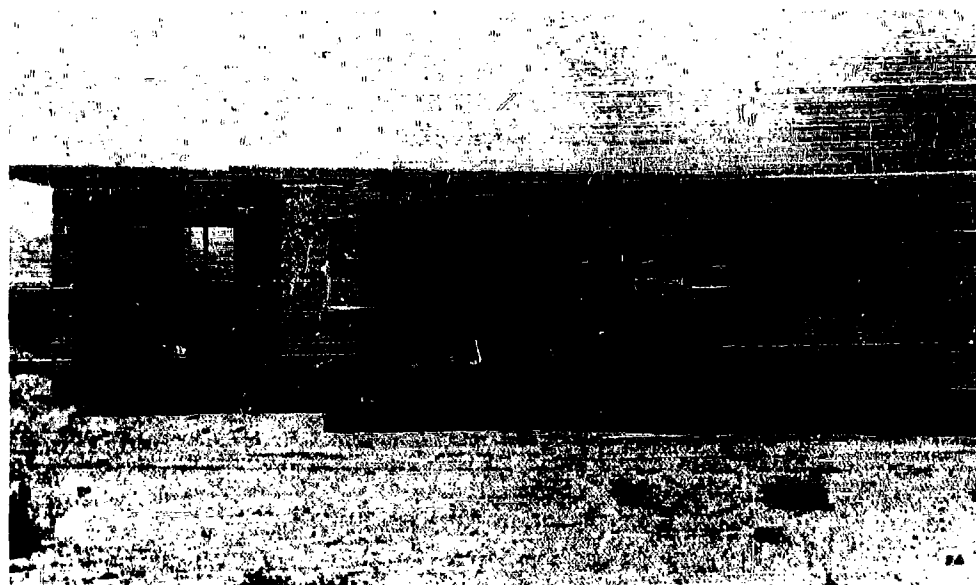


Figure 9. Photograph of Full-Size Precast Concrete Ranch House

building dimensions and the height of ceilings above floors were kept  $1/12$  of the full-size value, giving a model 40 inches long by  $27\frac{1}{2}$  inches wide with ceilings 8 inches high. Wall, partition, and roof thicknesses, however, were  $1/6$  of the full-scale values and were 1-inch thick compared to a calculated value of 1.02 inches for an equivalent electron density in steel. Room dimensions were thereby reduced by only  $1/2$  to  $3/4$  inches ( $1/2$  to  $3/4$  feet, full-scale) from true-scaled dimensions, because of the  $1/6$  wall-thickness scaling. The living room door and window of the full-scale building were blocked with  $3\frac{1}{2}$  inches of concrete block ( $151 \text{ lb/ft}^3$ ) for part of the experiments. One inch of steel was used for aperture blocking in the model. Each model wall and partition was of one-piece construction and was flame-cut to shape, including doors and windows. The roof was assembled by laying 9 strips of steel side by side on the top of the walls. The roof thus could easily be removed for placing or reading dosimeters without lifting more than 40 pounds at a time. The walls and partitions were supported on 1 inch-thick floor plates, representing 4 inches of poured concrete for the full-size building.

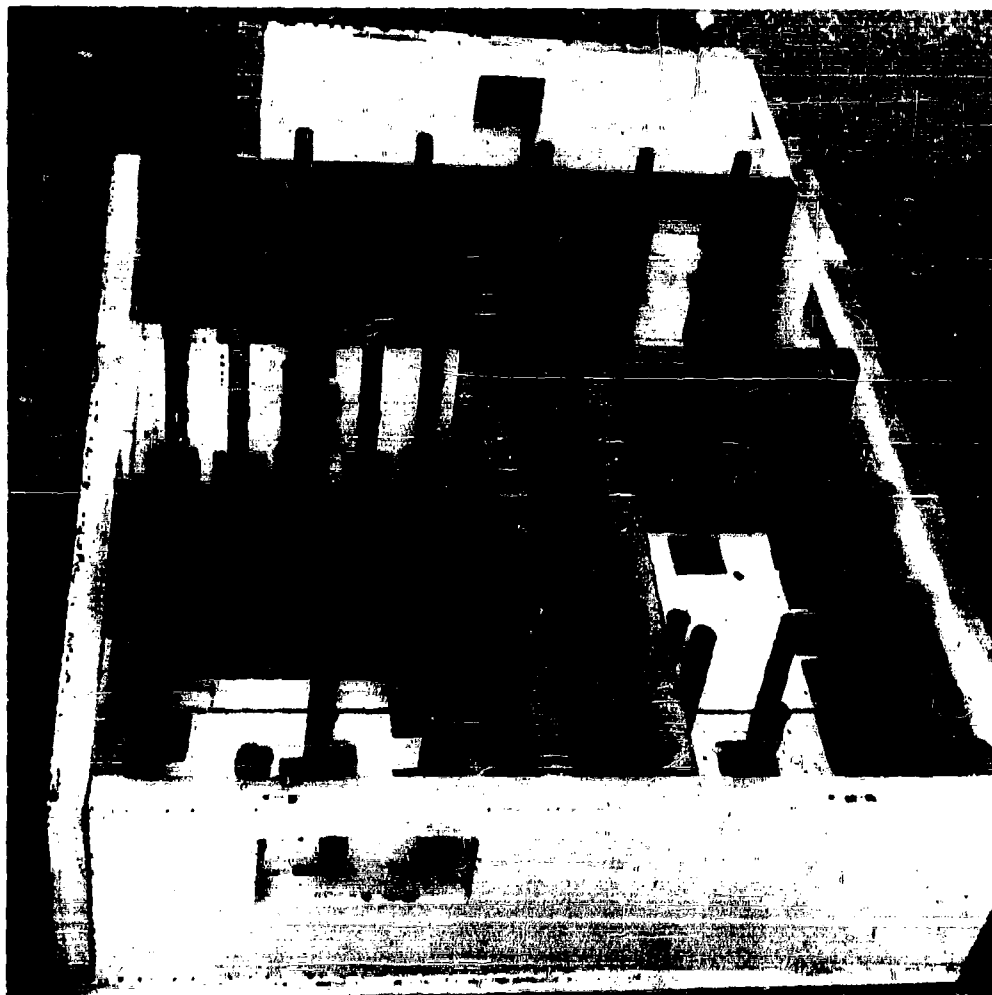


Figure 10. Model Precast Ranch House Showing Dosimeter Placement



## 2. Experimental Procedures

Procedures for conducting the ring experiments on the model precast concrete building ran as follows:

1. The model was assembled near the center of the test pad. The roof was left off to facilitate placement of dosimeters.
2. Polyethylene tubing was positioned as a source ring with the building at center. The ring radius was 25.5 inches for one series of experiments and 42.5 inches for a second series. Entrance and exit tubing was arranged for minimum ring discontinuity. Three tube loops, combined with ring entrance and exit bends of 6-inch radius, gave the best arrangement. Tubing was held in position with conduit nails driven into the test pad surface.
3. The source container was positioned 60 feet away from the experimental building. Ten feet of the polyethylene tubing between container and source ring were shielded with lead shot in canvas bags. The shielding began 6 inches from the source ring.
4. The hydraulic system was connected for dummy source runs. The container tube, with source, was by-passed with a special short-tube section. The dummy was placed in this short tube and the tube was connected to the pressure line (red fitting) running from the pump to the source ring lead. The dummy source was then pumped one or more times through the tubing to make certain that there was no chance of the real source becoming stuck or subjected to erratic motion.
5. Dosimeters were charged and placed at planned locations in the experimental building by clipping to stands made of paper base phenolic tubing with 1/32-inch walls.
6. The 1 inch-thick steel roof was placed on the experimental building.
7. Preparation was made for radiation runs. All personnel were equipped with direct-reading, 200-mr dosimeters and film badges. The area was monitored with survey meters and Technical Operations, Inc. Model 493 "Gammalarms." The hydraulic pumps were then turned off to relieve hydraulic pressure. Two men, equipped with survey meters, were used to prepare the source container for operation

(1)

and change fittings as necessary. One man performed the required operations, while the other monitored from a distance. Locks and positioning plugs were removed from each end of the tube containing the source, and a piston leather giving satisfactory dummy runs (item 4) was installed on the piston to assure that source motion would duplicate that obtained with the dummy. Tubing leads were then attached, with the pressure tube from the pump connected last as a safety precaution.

8. The 3-way solenoid valve control was switched to the by-pass position.

9. Both source clamps were retracted and the appropriate pump was turned on. The system was then ready for an experimental run with 10-curie, cobalt-60 source.

10. An observer equipped with a survey meter, a 20-power spotting scope, and a stop watch was stationed to monitor the run and the radiation area. He was in 2-way communication with a second person at the pump controls.

11. After a final check to see that the area was cleared of all personnel, the solenoid valve-control switch was thrown from by-pass position to source-circulation position. Exit of the source from the container switched the low-level (5 mr or less) signal (steady green light) of the "Gammalarms" to a high-level radiation signal (flashing red light). A timer attached to the "Gammalarms" gave a record of the time of exposure of the source.

12. After irradiation of the model, the source returned to the container. The solenoid valve was switched to the "by-pass" position, and the pump or pumps were then turned off. One person, with a survey meter, approached the container slowly and secured the source clamp on the return tube, thus locking the source in a position near the center of the container; the other man monitored these operations from a distance.

13. If another exposure were to follow, the four polyethylene tubes attached to the container would be removed. In this event, the return tube from the source ring was removed first, to relieve any residual pump pressure that might be acting on the source piston. The container was rotated 180 degrees and the four hoses were then connected to the container, 180 degrees from their original connections. After the last run for the day, positioning plugs were attached to the tube containing

the source and were locked in position. The four polyethylene tubes were left disconnected.

14. Exposed dosimeters were read and repositioned in the model house for the next exposure.

15. Temperature, atmospheric pressure, and relative humidity values were recorded in addition to dosimeter readings and exposure times.

### 3. Measurements and Results

The first series of experimental measurements on the 1/12-scale precast concrete house was made using a 42.5-inch radius source ring, thereby allowing comparison with the results of the experiments made on the full-scale building with a 42.5 foot radius source ring.<sup>6,7</sup> Table II presents a list of experiments performed on the model. For the first series of experiments, there was no simulated blocking in the living room door and windows.

One hundred 2r dosimeters were positioned within the model at the same relative positions as those used in the full-scale experiments. Considerable care was taken to see that the centers of the dosimeters were positioned at the correct height and horizontal location. For each run, the dosimeters were all mounted vertically or all mounted horizontally. Results of similar vertical and horizontal runs were compared to determine the effects of dosimeter orientation at the various dosimeter locations. Also, check runs were made with 24 dosimeters to determine if there were any detectable shielding caused by the large number of dosimeters and their stands. Figure 11 is a plan view of the model structure giving dosimeter locations by code number. Table III presents average normalized results of the refined experiments of this particular series. They are coded to locations shown in Figure 11.

The first two exposures of the model building were made with the source container only 2 feet away from the source ring. With this arrangement, the source, on leaving its container, was ten inches above ground level. The source was

<sup>6</sup>Auxier, Buchanan, Eisenhower, and Menker, op. cit.

<sup>7</sup>C. Eisenhower, "Analysis of Experiments of Light Residential Structures with Distributed Co<sup>60</sup> Sources," NBS, No. 6539, 15 October (1959).

TABLE II  
EXPERIMENTS PERFORMED ON THE MODEL PRECAST CONCRETE  
RANCH HOUSE

Description of Experiments	No. of Runs
A 42. 5-Inch Diameter Source Ring (3 Loops); No Aperture Blocking	
Runs with no lead shielding and with source container 2 feet from model building.	2
Source container 2 feet from model building, leads to source ring shielded with lead.	2
Source container 60 feet from model building; 10 feet of leads closest to building shielded; dosimeters both horizontal and vertical; exposure times from 350 - 800 sec.	5
A 42. 5-Inch Diameter Source Ring (3 Loops); Living Room Door and Window Blocked	
60-foot leads with 10 feet shielded; one inch blocking; horizontal and vertical dosimeters; exposure times from 741 - 764 sec.	3
Same, but 1 1/4-inch blocking.	2
A 25. 5-Inch Diameter Source Ring; 60 Foot Leads with 10 Feet Shielded	
Source ring consisting of one tubing loop; exposure time - 206 sec.	1
Source ring consisting of three tubing loops; horizontal and vertical dosimeters; exposure times from 216 - 454 sec.	4
Source ring consisting of five tubing loops; horizontal and vertical dosimeters; exposure times from 194 - 442 sec.	6

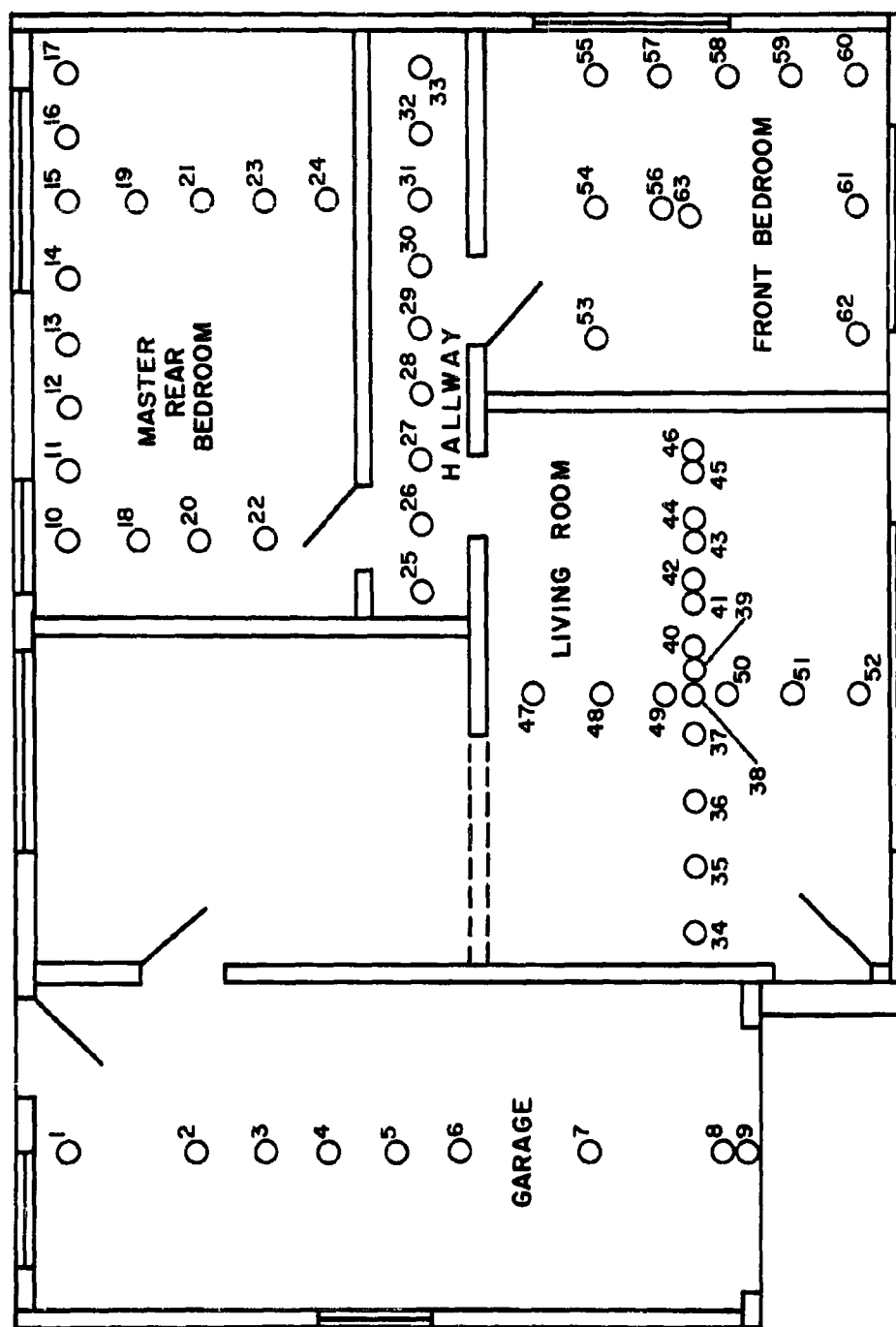


Figure 11. Floor Plan and Dosimeter Locations for the Precast Concrete Model Ranch House

TABLE III  
DOSE RATE DATA FOR PRECAST CONCRETE HOUSE  
(42.5 Foot-Radius Source Ring Simulated)

Dosimeter Position*	Full-Scale Data (Refs. 4 and 7)	Normalized Model Data†		Dosimeter Position*	Full-Scale Data (Refs. 4 and 7)	Normalized Model Data†	
		Vertical Dosim- eters	Horizontal Dosim- eters			Vertical Dosim- eters	Horizontal Dosim- eters
<b>Garage</b>				<b>22-b</b>	0.61	0.76	0.64
1-b	1.7	1.88	1.82	<b>23-b</b>	0.88	1.17	0.89
2-b	1.7	1.73	1.64	<b>24-b</b>	0.76	1.49	0.97
4-b	1.6	1.49	1.45	<b>Hallway</b>			
6-b	1.6	1.57	1.30	25-b	0.34	0.35	0.42
7-b	2.0	1.81	1.67	26-b	0.46	0.70	0.61
8-b	2.7	2.51	2.19	27-b	0.38	0.57	0.47
9-b	3.1	3.06	2.60	28-b	0.46	0.70	0.53
<b>Master Bedroom</b>				29-a	0.38	1.05	0.64
10-b	0.95	1.11	0.82	29-b	0.53	0.76	0.64
10-c	0.95	1.11	1.00	29-c	0.46	1.00	0.56
11-b	0.95	1.05	1.19	29-d	0.57	0.82	0.74
11-c	0.99	1.18	0.82	30-b	0.57	0.64	0.58
12-b	0.95	1.29	0.93	31-b	0.61	0.70	0.69
12-c	1.1	1.52	1.45	32-b	0.69	0.76	0.67
13-b	1.1	1.11	1.07	33-b	1.1	1.10	0.93
13-c	1.5	1.73	1.64	<b>Living Room</b>			
14-b	1.1	1.11	1.26	34-b	1.1	1.17	0.82
14-c	2.3	1.34	1.93	34-c	1.1	1.34	1.15
15-b	1.3	1.65	1.19	34-d	1.1	----	0.89
15-c	2.9	2.51	2.49	35-b	1.4	0.82	1.28
15-d	2.7	2.43	2.38	35-c	1.5	1.49	1.41
16-b	1.1	----	0.86	35-d	1.4	1.40	1.41
16-c	2.8	2.75	2.19	36-b	1.5	0.93	1.00
17-b	1.7	1.72	1.63	36-c	1.5	1.57	1.26
17-c	2.8	2.12	2.01	36-d	1.5	1.23	1.38
18-b	0.69	1.33	0.74	37-b	1.4	1.23	0.78
19-b	1.1	1.49	1.07	37-c	1.5	1.73	1.45
20-b	0.57	1.05	0.78	37-d	1.4	1.46	1.30
20-c	0.69	0.88	0.67	39-b	1.3	1.23	0.71
20-d	0.99	1.41	1.26	39-d	1.4	1.73	1.41
21-b	1.1	1.11	0.93				
21-c	1.3	1.57	1.64				

(Continued on next page)

TABLE III - (Continued)

DOSE RATE DATA FOR PRECAST CONCRETE HOUSE  
(42.5 Foot-Radius Source Ring Simulated)

Dosimeter Position*	Full-Scale Data (Refs. 4 and 7)	Normalized Model Data <sup>†</sup>		Dosimeter Position*	Full-Scale Data (Refs. 4 and 7)	Normalized Model Data <sup>†</sup>	
		Vertical Dosim- eters	Horizontal Dosim- eters			Vertical Dosim- eters	Horizontal Dosim- eters
Living Room (Cont'd.)				54-b	0.99	1.00	0.89
41-b	1.2	0.93	0.86	55-b	1.20	1.35	1.26
41-d	1.4	1.46	1.19	55-c	3.0	2.12	1.86
43-b	1.1	0.82	0.74	56-a	1.4	1.65	1.12
43-d	1.1	1.41	1.15	56-b	1.1	1.17	0.82
45-b	0.88	1.00	0.47	56-c	1.7	1.49	1.19
45-d	0.99	1.59	1.08	57-b	1.3	1.35	1.30
47-a	0.46	0.70	0.53	57-c	3.2	2.67	2.49
47-b	0.76	0.82	0.53	58-b	1.4	1.65	1.78
47-c	1.0	1.05	0.71	58-c	2.7	2.51	2.04
47-d	1.1	1.17	1.23	59-b	1.7	1.81	1.56
48-b	1.1	0.94	0.61	59-c	2.2	2.12	1.78
49-b	1.3	1.11	0.78	60-a	1.7	1.80	1.63
50-b	2.0	1.35	0.61	60-b	1.7	2.04	1.78
51-b	2.3	1.81	1.04	60-c	2.0	1.96	1.56
52-a	0.88	1.35	0.71	60-d	1.9	1.96	1.12
52-b	2.9	1.88	1.78	61-a	1.1	1.35	1.19
52-c	2.6	2.67	2.08	61-b	0.95	1.41	0.89
				61-c	3.0	2.51	2.38
				62-c	1.1	1.05	1.12
Front Bedroom				62-b	1.1	1.05	1.60
53-a	0.61	1.00	0.58	62-c	2.1	1.65	1.60
53-b	0.84	0.88	0.71				
53-c	0.92	1.23	0.74				

- \* a = 1 Foot Full-Scale or = 1 Inch Model Scale above Floor  
 b = 3 Foot Full-Scale or = 3 Inch Model Scale above Floor  
 c = 5 Foot Full-Scale or = 5 Inch Model Scale above Floor  
 d = 7 Foot Full-Scale or = 7 Inch Model Scale above Floor

<sup>†</sup>  $\frac{\text{MR/HR}}{2 \text{ MC/FT}}$  Full-Scale

(1)

channeled to ground level in a tight compound bend and then entered the source ring through a 6-inch radius. Return of the source from the ring followed the same pattern in reverse order. The measurements made for this arrangement showed that the radiation levels within the rooms facing the source container and its leads were high, because of the exposure while the source was in the leads. Shielding of the leads from the container to the source ring only partially succeeded in reducing the high readings.

All subsequent runs of this and other series on the precast model house were made with the source container 60 feet away from the model and with leads covered with bags of lead shot to within 6 inches of the source ring. Leads were shielded for a total distance of 10 feet after which they were partially hidden behind the shielding for an additional 30 feet.

Source handling of the 10 curies in the leads proved to be critical because of the very short—3 to 10 minutes—exposure required to obtain satisfactory readings on the 2r dosimeters. Only a few seconds' extra exposure by the source while in the leads close to the source ring could give a noticeable additional dose to the rooms facing the leads. To overcome this, a metering pump was set to give the desired source speed through the source-ring tubing. Both the gear pump and the preset metering pump were turned on in the by-pass condition. The gear pump was then used to move the source through the leads and under the shield at high speed. A little experimentation established a technique of switching to the metered pump so that the source left the shield to enter the ring at the properly reduced speed. This operation was observed from a distance with a spotting scope, thus allowing accurate exposure timing from the emergence of the source from the shielded section of leads and its return to this section. As soon as the source returned to the shielded area, the gear pump was again turned on to deliver the source to the container rapidly.

With this technique, five runs were made for the 42.5 inch-radius ring experiments without blocking. In most of the runs, the source was successfully switched to slow speed as the source piston and leader were emerging from the shielded tubing or before the source entered the source ring. Occasionally, the source entered the ring before slowing down. On these rare occasions, the dosimeters had to be recharged and the run repeated.



During the 5 runs, exposure time was also varied from 350 to 800 seconds to obtain readings that were above 20 per cent of the rated dosimeter value for all locations. Short runs were made to keep readings near windows and doors below 80 per cent of full-scale deflection. Longer runs raised dose levels in the hallway of the model well above the low range for the dosimeters. No difficulty was observed in duplicating the normalized dose rates from runs of different timing and dose levels, as long as dosimeter readings were between 10 and 90 per cent of full-scale. The average normalized results for the 5 runs, including both vertically and horizontally mounted dosimeters, are given in Table III along with comparable full-scale data.

Additional runs with the 42.5-inch radius source ring were made with the living room picture window and door blocked with one inch of steel, using the refined source-delivery technique just cited. The average normalized results of these runs are tabulated in Table IV for both vertical and horizontal dosimeters. Comparable full-scale data for this experiment is also given. Results are not given for two experiments with 1-1/4 inch blocking, because of faulty source delivery while trying a different delivery procedure.

Eleven runs were made on the 1/12-scale precast concrete model house with a 25.5 inch-radius source ring for comparison with data on the full-size building with a 25.5 foot-radius source ring. For this series of experiments, there was no blocking in any of the windows or doors. Proper delivery of the source to the source ring was more critical with this smaller radius ring, because shorter run times (200 to 400 seconds) were required since the source was closer to the building.

Exposures were made with rings composed of 1, 3, and 5 tubing loops to determine the optimum number of loops for this series of runs with the source very close to the building. Eleven runs were made using the source-delivery techniques that had worked best for the 42.5 inch-radius ring experiments, i. e., long shielded leads. A source ring comprised of 3 spiraled loops represented the best compromise arrangement. One loop, as expected, gave unsatisfactory results because of increased sensitivity to both source delivery and ring discontinuity; the latter was caused by entrance and exit of the leads from the source ring. Source rings comprised of 5 loops greatly reduced the sensitivity to source delivery and to the

TABLE IV  
DOSE RATE DATA FOR PRECAST CONCRETE HOUSE  
(42.5 Foot-Radius Source Ring Simulated, Living Room Door and  
Window Blocked with 3-1/2 Inch-Thick Cement)

Dosimeter Position*	Full-Scale Data (Refs. 4 and 7)	Normalized Model Data†		Dosimeter Position*	Full-Scale Data (Refs. 4 and 7)	Normalized Model Data†	
		Vertical Dosim- eters	Horizontal Dosim- eters			Vertical Dosim- eters	Horizontal Dosim- eters
Garage				Hallway			
1-b	1.83	2.05	1.85	25-b	0.31	0.48	0.42
3-b	1.77	1.64	1.51	26-b	0.44	0.51	0.50
5-a	1.35	1.45	1.35	27-b	0.35	0.63	0.60
5-b	1.67	1.49	1.25	28-b	0.42	0.49	0.49
5-c	1.67	1.62	1.53	29-a	0.31	0.60	0.59
5-d	2.29	2.23	2.06	29-b	0.52	0.52	0.50
7-b	2.21	2.17	1.98	29-c	0.48	0.55	0.50
				30-b	0.50	0.61	0.61
Master Bedroom				31-b	0.56	0.67	0.70
10-b	1.00	0.84	0.80	32-b	0.62	0.73	0.94
10-c	0.96	1.09	0.82	33-b	1.02	1.07	1.08
11-b	1.04	1.00	0.90	Living Room			
11-c	1.00	0.96	1.16	34-b	0.69	0.77	0.77
12-b	1.04	0.90	0.86	34-c	0.69	0.93	0.82
12-c	1.10	1.34	1.20	34-d	0.69	0.69	0.64
13-b	1.15	1.10	1.03	35-b	0.69	0.80	0.71
13-c	1.56	1.56	1.61	35-c	0.75	0.82	0.73
14-b	1.04	1.17	1.14	35-d	0.75	0.96	0.86
14-c	2.71	2.25	1.91	36-b	0.69	1.10	0.95
15-b	1.31	1.22	1.16	36-c	0.77	0.96	0.94
15-c	3.04	2.80	2.52	36-d	0.87	0.96	0.94
15-d	2.83	2.11	2.30	37-b	0.75	0.93	0.86
16-b	1.42	Bad Dosimeter		37-c	0.75	1.03	0.94
16-c	2.06	2.27	2.26	37-d	0.77	0.86	0.73
17-b	1.75	1.83	1.72	38-a	0.37	0.69	0.64
17-c	2.06	1.88	1.98	38-b	0.75	0.82	0.73
20-b	0.69	0.70	0.63	38-c	0.79	0.98	1.03
20-c	0.75	0.73	0.67	38-d	0.79	0.74	0.73
20-d	1.25	1.17	1.07	40-b	0.71	0.82	0.64
21-b	1.15	1.04	0.94	40-d	0.79	0.88	-----
21-c	1.33	1.78	1.40				
21-d	1.98	1.59	1.48				
24-d	1.35	1.37	1.23				

(Continued on next page)

TABLE IV - (Continued)

**DOSE RATE DATA FOR PRECAST CONCRETE HOUSE**  
**(42.5 Foot-Radius Source Ring Simulated, Living Room Door and**  
**Window Blocked with 3-1/2 Inch-Thick Cement)**

Dosimeter Position*	Full-Scale Data (Refs. 4 and 7)	Normalized Model Data†		Dosimeter Position*	Full-Scale Data (Refs. 4 and 7)	Normalized Model Data†	
		Vertical Dosim- eters	Horizontal Dosim- eters			Vertical Dosim- eters	Horizontal Dosim- eters
Living Room (Cont'd.)				55-b	1.25	1.25	1.29
42-b	0.67	0.63	0.70	55-c	2.75	2.62	2.39
42-d	0.75	0.71	0.95	56-a	0.90	1.07	1.03
44-b	1.37	0.71	0.67	56-b	1.08	1.24	1.03
44-d	0.73	0.80	0.80	56-c	1.94	2.01	1.05
46-b	2.12	0.73	0.61	57-b	1.25	1.29	1.31
46-d	0.62	0.73	0.86	57-c	2.98	2.81	2.58
47-a	0.33	0.56	0.56	58-b	1.25	1.34	1.31
47-b	0.52	0.62	0.56	58-c	2.60	2.42	2.28
47-c	0.69	0.56	0.56	59-b	1.56	1.59	1.57
48-b	0.54	0.76	0.86	59-c	2.12	2.00	1.98
49-b	0.71	0.70	0.67	60-a	1.62	1.85	1.83
50-b	1.10	0.86	0.77	60-b	1.62	1.89	1.85
51-b	0.94	1.19	1.14	60-c	1.87	1.92	1.89
52-a	0.46	0.84	0.77	60-d	1.83	1.68	1.64
52-b	1.17	0.92	0.86	61-a	1.33	1.32	1.29
52-c	1.04	1.03	1.05	61-b	1.29	Bad Dosimeter	
				61-c	2.71	2.60	2.39
				62-a	1.04	1.03	0.90
Front Bedroom				62-b	1.08	0.86	0.90
53-a	0.65	0.81	0.90	62-c	1.98	1.50	1.40
53-b	0.75	0.64	0.57	63-a	0.90	1.13	0.88
53-c	0.79	0.74	0.67	63-b	1.04	0.94	0.84
54-b	1.02	0.82	0.80	63-c	1.94	1.49	1.22

- \* a = 1 Foot Full-Scale or = 1 Inch Model Scale above Floor  
 b = 3 Foot Full-Scale or = 3 Inch Model Scale above Floor  
 c = 5 Foot Full-Scale or = 5 Inch Model Scale above Floor  
 d = 7 Foot Full-Scale or = 7 Inch Model Scale above Floor

†  $\frac{\text{MR/HR}}{2 \text{ MC/FT}}$  Full-Scale

(7)

discontinuity caused by the leads; however, the source ring width (2.5 inches) was becoming appreciable and caused the ring to assume a slightly rectangular shape to avoid the building corners. Average normalized results for 2 runs with vertical and 2 with horizontal dosimeters, as well as full-scale data, are given in Table V for a source ring consisting of 3 spiraled loops of polyethylene tubing.

#### 4. Discussion of Model Results

Rapid delivery of the 10-curie source, combined with shielding of the leads to the ring, was required for ring experiments on the 1/12-scale model of the precast concrete house. This was necessitated by the short exposures of only 3 to 10 minutes required with the source rings 25.5 and 42.5 inches from the center of the building. Considerable effort was expended refining the technique for delivery of the source to the ring to assure exposure from the ring alone. The following is a discussion of results obtained with the high-speed, source-delivery techniques described earlier in this report.

Data in general agrees well with the full-scale data except for a few specific discrepancies. These are related to the relatively large size of the dosimeters and/or to the relatively thicker walls in the model. The Landsverk L-81 dosimeter used, even though only 1-1/2 inches long, represents an equivalent dosimeter length of 18 inches in a full-scale building. This is 3 times the length used in full-scale building experiments. If model measurements were made at points of steep gamma-ray dose rate gradients, discrepancies might be expected. In this series of tests, dosimeter locations in the model building are governed by the locations picked for the full-scale runs. Without predetermined positions for dosimeters, original model work could be done with dosimeters placed in positions more suited to their size. The building dimensions were scaled by a factor of 12, except for the walls, which were governed by the model material used. For the present series of tests, steel was used, giving a wall thickness 1/6 that of a full-scale concrete building. These relatively thicker walls gave slightly smaller direct line-of-sight angles from the source through wall openings than for a full-scale test, thereby giving some distortion to the gamma-ray field in the model building. These discrepancies, as well as illustrations of typical agreement between the model and full-scale data,

TABLE V

**DOSE RATE DATA FOR PRECAST CONCRETE HOUSE**  
**(25.5 Foot-Radius Source Ring Simulated)**

Dosimeter Position*	Full-Scale Data (Refs. 4 and 7)	Normalized Model Data†		Dosimeter Position*	Full-Scale Data (Refs. 4 and 7)	Normalized Model Data†	
		Vertical Dosim- eters	Horizontal Dosim- eters			Vertical Dosim- eters	Horizontal Dosim- eters
Garage				Hallway			
1-b	4.26	5.35	5.23	25-b	0.43	0.53	0.91
3-b	3.32	3.80	3.93	26-b	0.60	0.56	0.91
5-a	1.15	3.23	3.20	27-b	0.51	0.83	0.91
5-b	3.40	3.41	3.89	28-b	0.55	0.63	0.74
5-c	3.62	3.41	3.55	29-a	0.43	0.53	0.55
5-d	3.15	3.41	3.33	29-b	0.72	0.92	0.91
7-b	4.64	4.91	4.75	29-c	0.64	0.89	0.94
				29-d	0.60	1.09	1.13
Master Bedroom				30-b	0.85	1.02	1.30
10-b	1.62	1.59	1.59	31-b	1.06	1.19	1.42
10-c	1.49	1.55	1.69	32-b	1.40	1.84	1.64
11-b	1.70	2.03	2.16	33-b	2.55	2.48	2.55
11-c	1.70	1.65	1.77				
12-b	1.91	2.12	1.82	Living Room			
12-c	1.74	2.65	1.99	34-b	1.45	1.72	1.96
13-b	2.19	2.12	2.59	34-c	2.13	1.52	1.62
13-c	2.00	2.17	2.51	34-d	2.00	1.78	2.12
14-b	2.55	2.92	2.68	35-b	1.70	1.45	1.49
14-c	3.40	----	----	35-c	2.94	1.68	----
15-b	2.98	3.27	3.18	35-d	2.64	2.30	2.25
15-c	4.68	4.69	4.80	36-b	1.62	1.59	1.77
16-b	3.49	4.07	3.72	36-c	2.81	1.81	1.77
16-c	4.89	4.29	4.58	36-d	2.77	2.56	2.68
17-b	4.13	5.17	4.93	37-b	1.49	1.59	1.64
17-c	4.47	4.12	4.41	37-c	2.77	1.62	1.62
20-b	0.85	----	----	37-d	2.68	2.44	2.50
20-c	1.11	1.33	1.20	40-b	1.28	1.29	1.56
20-d	1.02	1.59	1.43	40-c	2.43	1.86	1.56
21-b	2.34	2.57	2.60	40-d	2.55	2.44	2.51
21-c	2.04	2.83	2.77	42-b	1.28	1.45	1.46
21-d	2.34	2.12	1.99	42-c	2.55	1.64	1.56
24-d	1.45	1.65	1.69	42-d	2.36	2.43	2.55

(Continued on next page)

TABLE V -- (Continued)

DOSE RATE DATA FOR PRECAST CONCRETE HOUSE

(25.5 Foot-Radius Source Ring Simulated)

Dosimeter Position*	Full-Scale Data (Refs. 4 and 7)	Normalized Model Data†		Dosimeter Position*	Full-Scale Data (Refs. 4 and 7)	Normalized Model Data†	
		Vertical Dosim- eters	Horizontal Dosim- eters			Vertical Dosim- eters	Horizontal Dosim- eters
Living Room (Cont'd.)							
44-b	1.15	1.09	1.17	54-b	2.09	2.00	1.86
44-c	2.04	1.59	1.46	55-b	2.98	2.73	3.07
44-d	1.96	2.12	2.34	55-c	4.77	2.83	3.50
46-b	1.06	1.02	1.07	56-a	0.98	1.59	1.49
46-c	1.70	1.39	1.42	56-b	2.43	2.26	2.42
46-d	1.70	1.59	1.64	56-c	2.30	1.96	1.92
47-a	0.43	0.76	0.58	56-d	----	2.04	2.16
47-b	0.98	0.89	0.97	57-b	3.15	2.73	2.81
47-c	1.70	1.19	1.30	57-c	5.32	2.96	3.07
47-d	1.91	1.29	1.30				
48-b	1.11	1.06	1.13	58-b	3.32	3.32	3.81
				58-c	5.11	2.83	2.98
49-b	1.40	1.45	1.56				
50-b	2.13	1.68	1.73	59-b	4.17	3.23	3.98
				59-c	3.40	3.05	3.20
51-b	4.13	1.79	2.51	60-a	7.23	6.46	6.31
52-a	1.91	2.12	2.12	60-b	4.43	3.54	4.02
52-b	5.74	2.65	2.08	60-c	3.19	2.79	3.03
52-c	5.06	3.81	4.76	60-d	2.38	2.43	2.98
52-d	5.11	3.89	4.07	61-b	3.32	3.45	3.03
				61-c	5.53	3.81	3.37
Front Bedroom				62-b	2.43	2.74	2.34
53-a	0.61	0.43	0.63				
53-b	1.28	1.26	1.49				
53-c	1.49	1.42	1.62				
53-d	----	1.36	1.56				

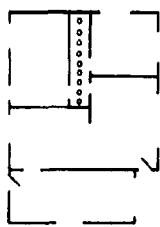
\* a = 1 Foot Full-Scale or = 1 Inch Model Scale above Floor  
 b = 3 Foot Full-Scale or = 3 Inch Model Scale above Floor  
 c = 5 Foot Full-Scale or = 5 Inch Model Scale above Floor  
 d = 7 Foot Full-Scale or = 7 Inch Model Scale above Floor

†  $\frac{\text{MR/HR}}{2 \text{ MC/FT}}$  Full-Scale

are shown in Figures 12 through 25. These figures are plots of part of the normalized data previously presented in Tables III, IV, and V, for experiments with both the 25.5 and 42.5 inch-radius source rings. Curves are presented in each figure for model results with both horizontal and vertical dosimeters, comparable full-scale values, and calculated transparent-house values. Figures 12 through 14 present data for the 42.5-inch ring source experiments without living room door and window blocking, while Figures 15 through 19 show comparable results with blocking. Figures 20 through 25 are curves of normalized data taken from experiments with a 25.5-inch source ring without aperture blocking.

Horizontal traverses in the hallway are plotted in Figures 12, 16, and 21 for each of the three experiments. In each case, measured model values were in the order of 20 per cent higher than the full-scale data, although for the 42.5 inch-radius source ring without blocking (Figure 12), even higher values were obtained toward the center of the building where three doors opened into the hallway. This general 20 per cent increase in model values over the full-scale results may be caused by using a wall thickness of 1.0 inch to match electron density instead of 1.2 inches to match the weight per unit area of the concrete wall. This difference in thickness should be especially noticeable in the hallway, because a sizable percentage of the gamma ray reaching it passes through two or more walls, each of which is 17 per cent thinner than the calculated mass thickness. Additionally, since the dimensions of the corridor are of the same order as the mean free path of 1.25 mev gamma rays in steel, inaccuracies may be introduced into the experiment by so-called "edge effects." Edge effects, in general, do not scale in the same manner as broad-beam penetration effects. For the 42.5-inch source ring experiment, without blocking, the model hallway data follows the same contour as the full-size results. It should be noted, however, that with blocking the model contour changes appreciably. The full-scale hallway dose rate contour and values remained nearly the same with or without blocking with readings 0 to 5 per cent lower in the hall doorway area (that area that is subjected to the radiation entering the living room door and window) and 10 per cent lower in the outer part of the hallway, which is least affected by radiation coming from the living room. The gamma-ray dose in the model hallway with the living room window and door blocked decreased approximately 10 per cent in the inner half of the hallway and none in the outer half. The dose decreased most in the

DOSIMETER POSITIONS FOR FIGURE 12



—○— FULL SCALE DATA  
 ---□--- NORMALIZED MODEL DATA - VERTICAL DOSIMETERS  
 ---△--- NORMALIZED MODEL DATA - HORIZONTAL DOSIMETERS

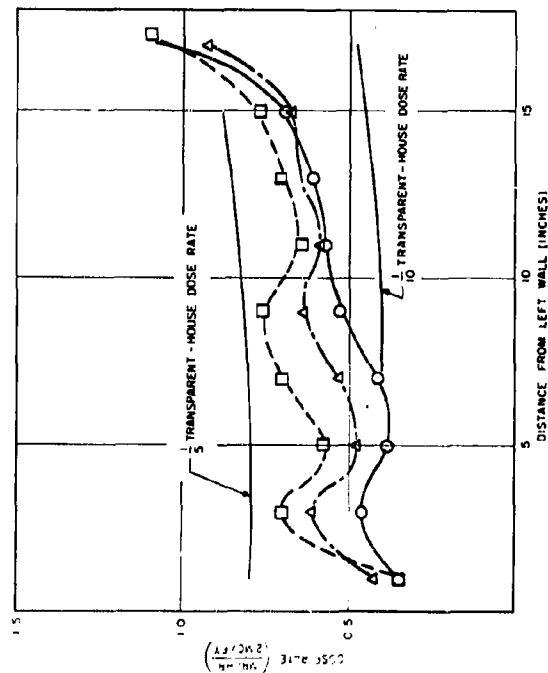


Figure 12. Precast Concrete House, Horizontal Traverse along Hallway 3 Inches above Floor; 42.5-Inch Source Radius

DOSIMETER POSITIONS FOR FIGURE 13

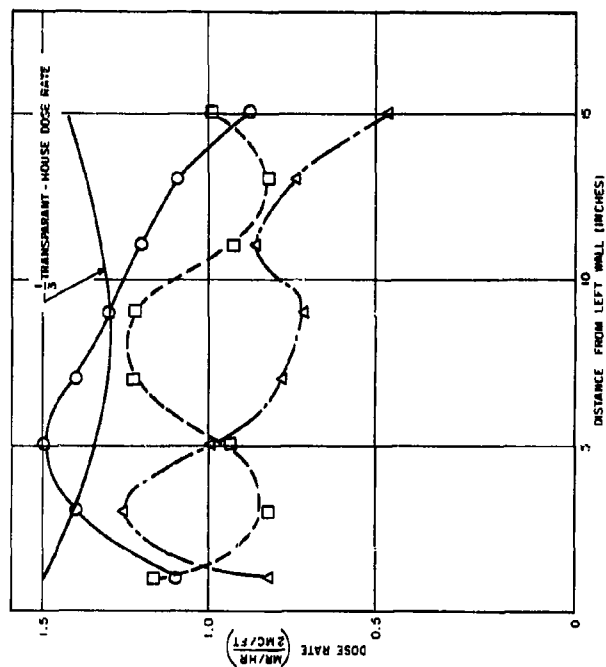
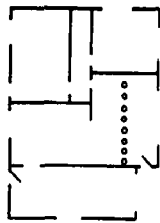


Figure 13. Precast Concrete House, Horizontal Traverse along Centerline of Living Room 3 Inches above Floor; 42.5-Inch Source Radius



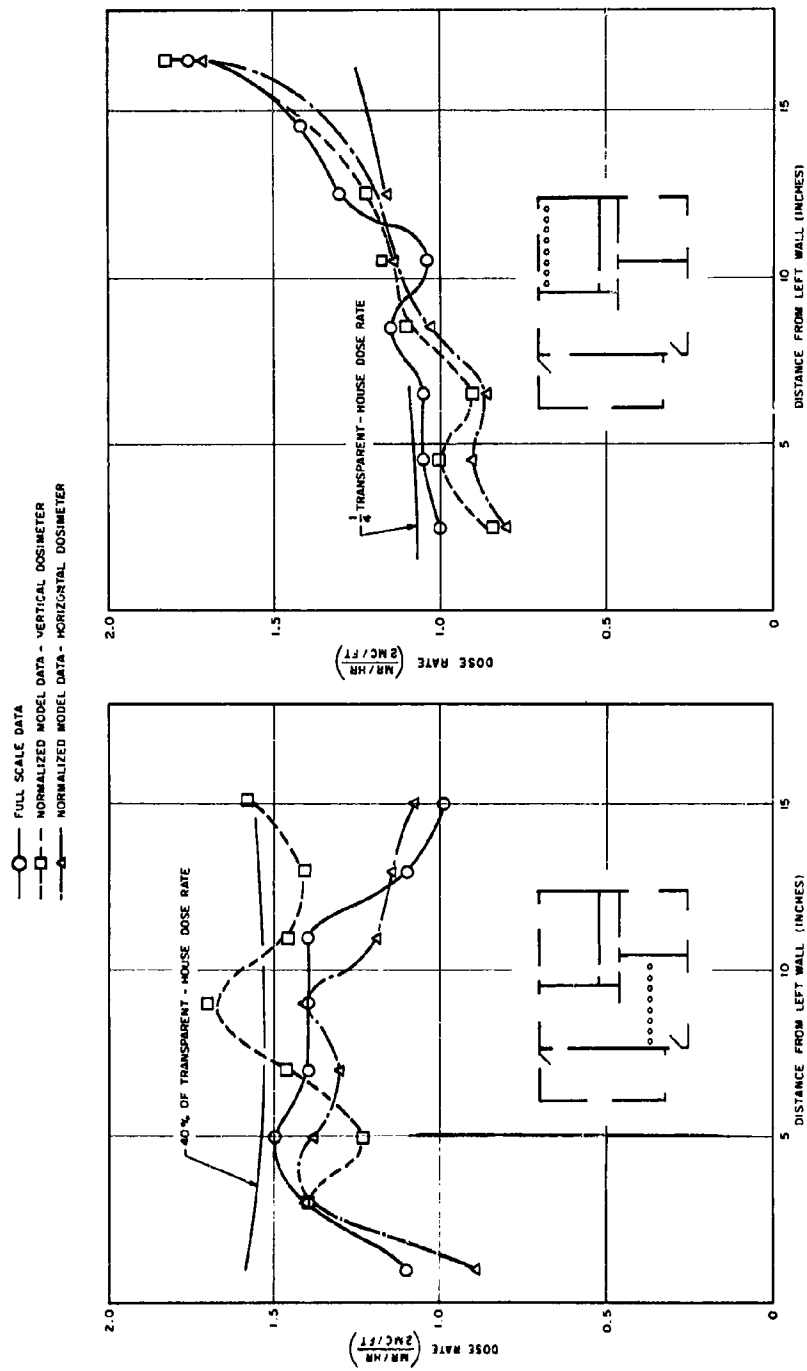


Figure 14. Precast Concrete House, Horizontal Traverse along Centerline of Living Room 7 Inches above Floor; 42.5-Inch Source Radius

Figure 15. Precast Concrete House, Horizontal Traverse along Rear Wall of Master Bedroom 3 Inches above Floor; 42.5-Inch Source Radius

○ FULL SCALE DATA  
 □ NORMALIZED MODEL DATA - VERTICAL DOSIMETER  
 △ NORMALIZED MODEL DATA - HORIZONTAL DOSIMETER

DOSIMETER POSITIONS FOR FIGURE 16

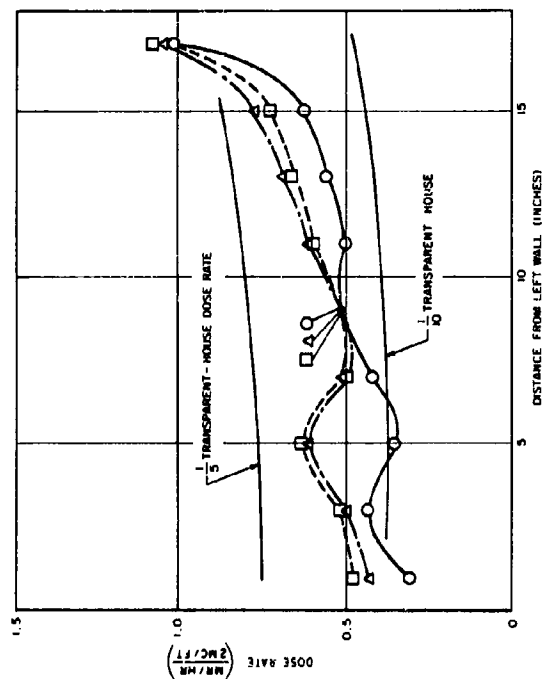
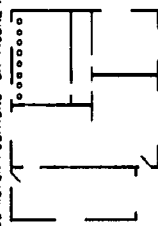


Figure 16. Precast Concrete House, Horizontal Traverse along Hallway 3 Inches above Floor; 42.5-Inch Source Radius

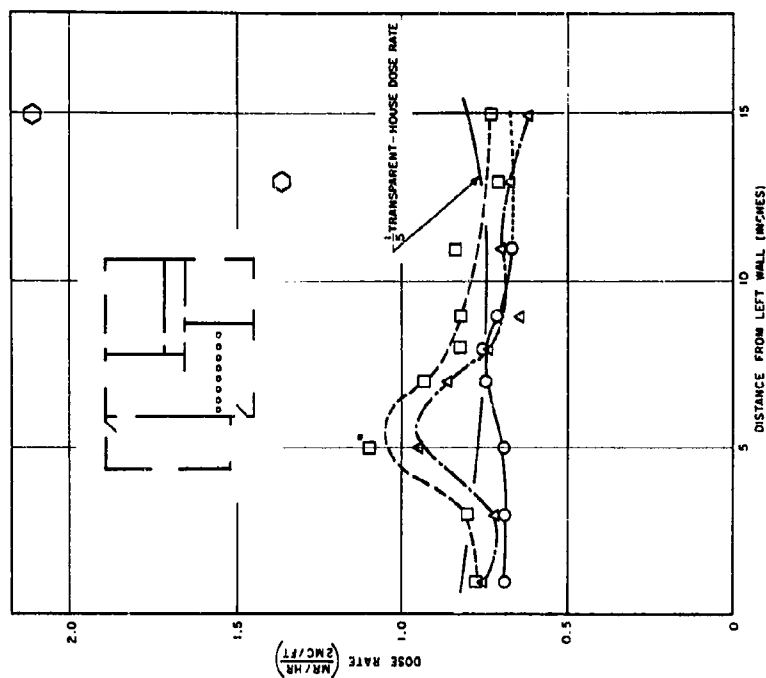
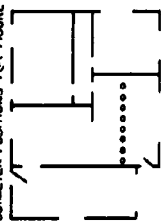
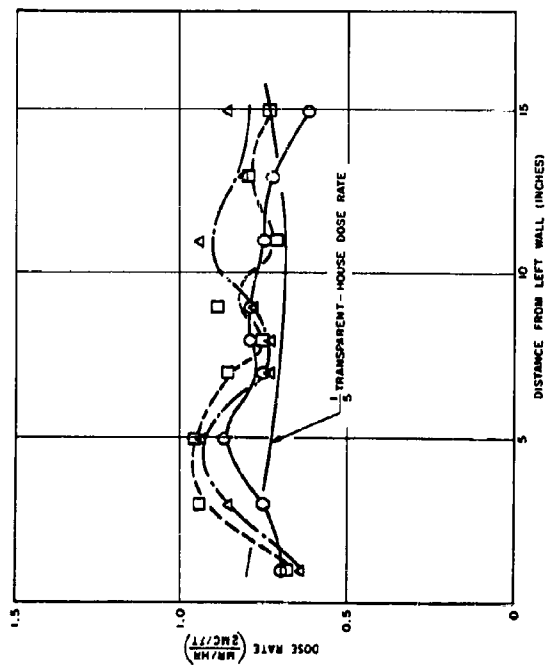


Figure 17. Precast Concrete House, Horizontal Traverse along Living Room 3 Inches above Floor; 42.5-Inch Source Radius

DOSIMETER POSITIONS FOR FIGURE 18



—○— FULL SCALE DATA  
 ---□--- NORMALIZED MODEL DATA - VERTICAL DOSIMETER  
 ---△--- NORMALIZED MODEL DATA - HORIZONTAL DOSIMETER



DOSIMETER POSITIONS FOR FIGURE 19

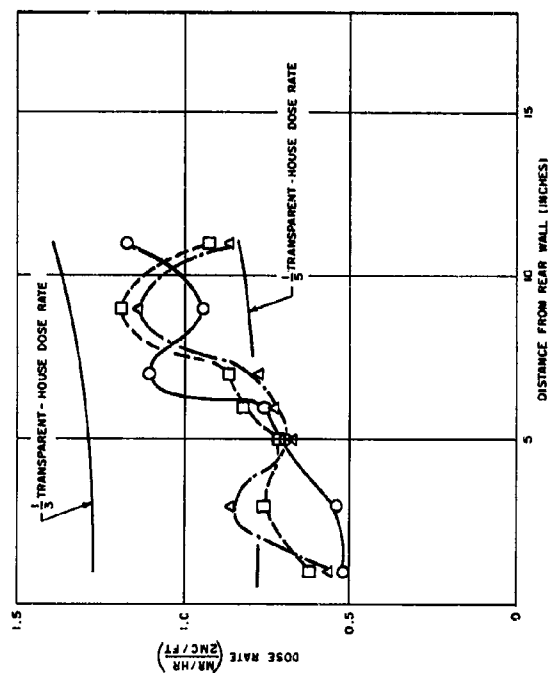


Figure 18. Precast Concrete House, Horizontal  
 Traverse along Living Room 7 Inches above Floor;  
 42.5-Inch Source Radius

Figure 19. Precast Concrete House, Horizontal  
 Traverse from Back to Front of Living Room  
 3 Inches above Floor; 42.5-Inch Source Radius

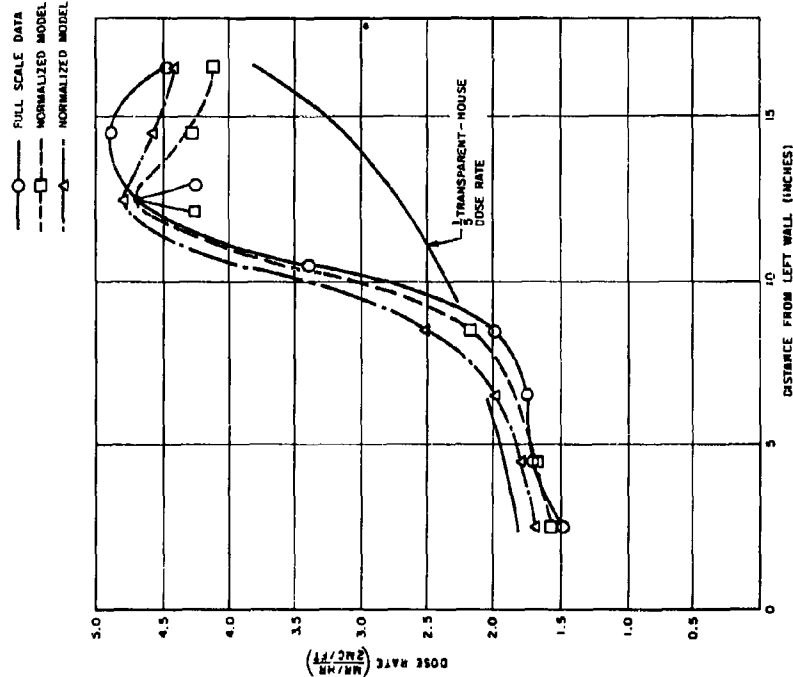


Figure 20. Precast Concrete House, Horizontal Traverse along Rear Wall of Master Bedroom 5 Inches above Floor; 25.5-Inch Source Radius

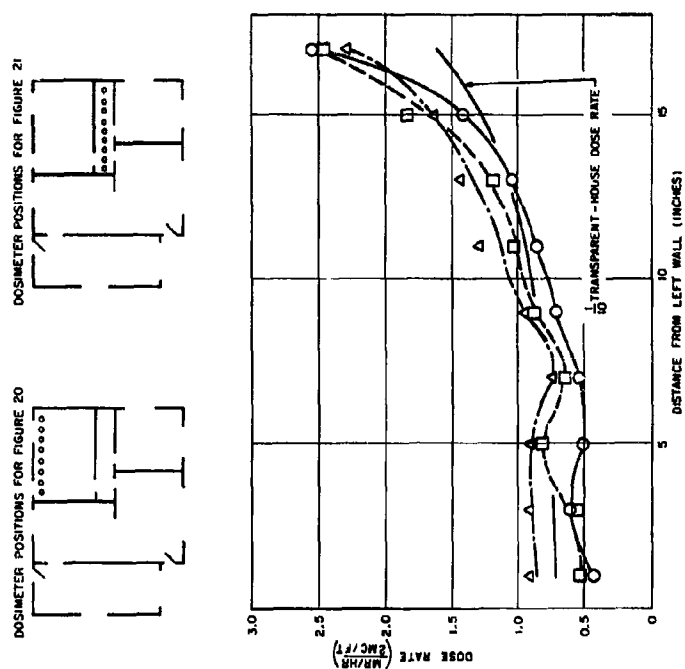


Figure 21. Precast Concrete House, Horizontal Traverse along Hallway 3 Inches above Floor; 25.5-Inch Source Radius

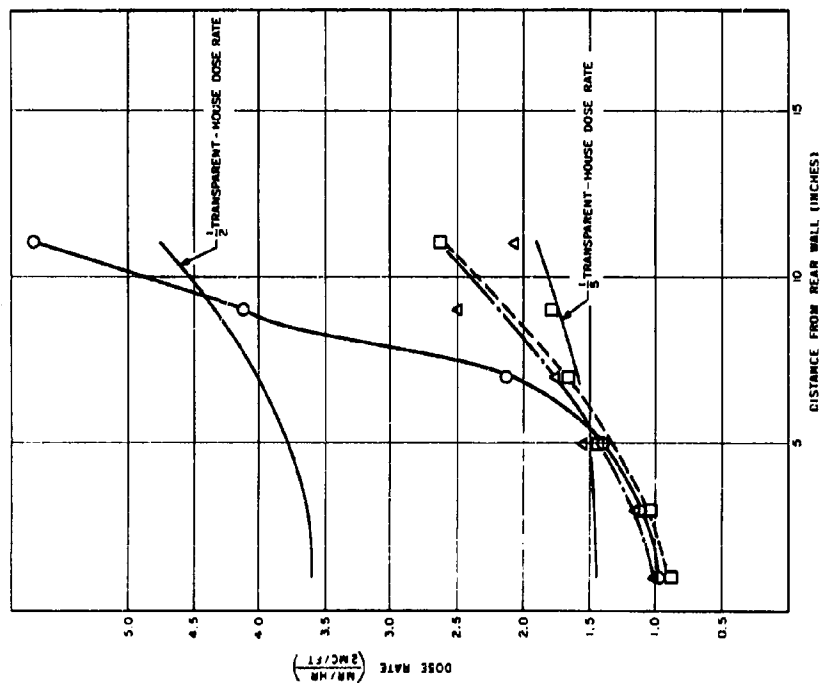


Figure 22. Precast Concrete House, Horizontal Traverse from Back to Front of Living Room 3 inches above Floor; 25.5-Inch Source Radius

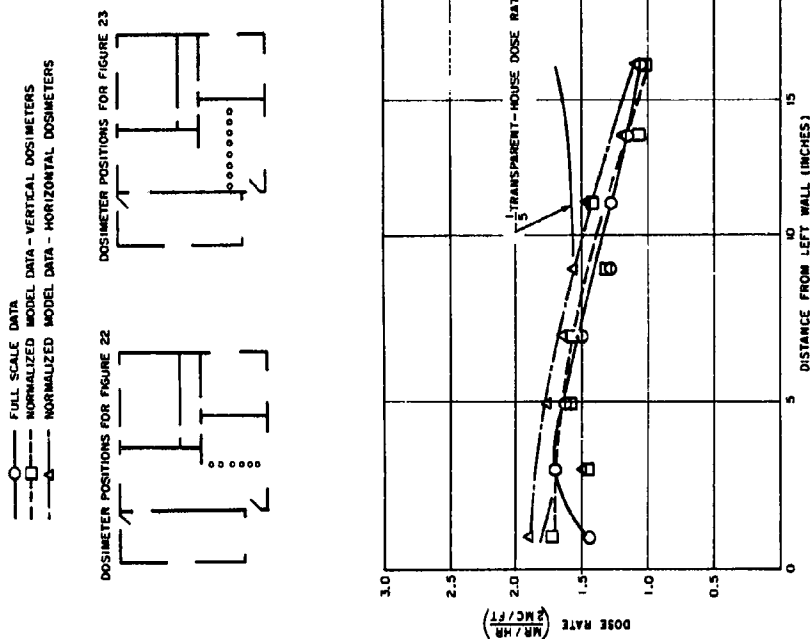


Figure 23. Precast Concrete House, Horizontal Traverse along Centerline of Living Room 3 inches above Floor; 25.5-Inch Source Radius

2



2



region of direct line-of-sight between the source, living room outside door, and the living room hallway door. Blocking the living room outside door, as well as the window, effected more reduction of dose in the adjacent hallway of the model than in the full-scale tests. No blocking effect was observed for the model in the outer part of the hallway, which is also farthest away from the living room. For the full-scale structure, most of the blocking effect seemed to be in this region. The dose rate in the hallway of the full-scale and model buildings, with 42.5-foot and 42.5-inch source rings respectively, lies between  $1/10$  and  $1/5$  of the gamma-ray dose that would have been measured if the building mass were removed, i. e., transparent-house dose rate. For experiments with the 25.5-inch and 25.5-foot source rings, the dose rate in the hallway lies between  $1/20$  and  $1/8$  of the transparent house value. The greater shelter factor present with the smaller source-ring diameter is largely attributable to the greater contribution to shielding by that portion of the floor slab substantially above grade level. The closer the source ring is to the raised floor slab, the greater will be the attenuation of the floor slab. Figures 19 and 22 contain horizontal traverses from the rear to the front of the living room at the three-foot level for the 42.5 inch source ring with blocking for the 25.5-inch case respectively. Figure 22 shows very graphically the extreme differences which can be obtained between full-scale tests and model tests because of dosimeter-size difference combined with the increased thickness of the wall in the model. The dosimeters in the full-scale house at the 3-foot level are located so that every part of each dosimeter is slightly above the bottom of the picture window. The two dosimeters in front received a sizable direct-beam dose with little shielding effect from the window ledge. For the scale model, the vertical dosimeters extend below the window ledge. This, coupled with the thicker wall, puts most of the front dosimeters in the shadow of the wall below the window as far as line-of-sight radiation is concerned. For the horizontal dosimeters, the effect was about the same, even though the diameter of the dosimeters represents 6 inches, or the height of the dosimeters used in the full-scale tests. In this case, most of the effect was attributable to the relatively thicker model wall changing line-of-sight angles, and to the increased wall thickness pushing the dosimeter location farther into the interior of the room. The sensitivity of the dosimeters to minor height variations at the two positions in front was very severe, because of the high dose rate gradient

①

in this region. For the 42.5 inch-radius experiments, the dose rate in the living room was approximately cut in half by blocking the living room outside door and the picture window. Comparison of dose contours from back to front of the living room with the blocking (Figure 19) shows that the dose-rate contour has been altered or offset by scaled dimensional errors, caused by relatively greater wall thickness. In this case, direct line-of-sight radiation passing through the open rear door of the garage, through the kitchen door, and thence into the living room through the archway, will strike the dosimeters differently as the dimensions are altered by the presence of the thicker walls.

Horizontal traverses along the centerline of the living room illustrate graphically the variations caused by thicker walls and relatively large dosimeters. Figure 13 shows that for the 42.5-inch source ring, without window blocking, the model was very sensitive to the high dose-rate gradient present at the 3-foot level. At the 7-foot level (Figure 14), this sensitivity was greatly reduced, because the gradient is less steep at this level. With the window and door blocked, model results agree quite well with the full-scale results (see Figures 17 and 18). With the 25.5 inch-radius source ring, the large gradient is above the top of the L-81 dosimeters at the 3-foot level, as shown in Figure 23. However, the steep gradient region has been elevated just enough to reduce the 5-foot level readings 50 per cent, as shown in Figure 24. At the 7-foot level, the dosimeters are once again out of the gradient, as shown in Figure 25 by the excellent agreement between model and full-scale results. Typical results in the rear or master bedroom are illustrated in Figures 15 and 20. In this room the windows were higher above the floor than the living room window, so that the tops of the 3-foot level dosimeters were only slightly above the window ledge for model tests. Those dosimeters were mostly out of the high gradient and gave results (see Figure 15) that compared within 20 per cent of the full-scale results. At the 5-foot level, as shown in Figure 20, the agreement was excellent. The dosimeters in the model were at just the right height in the window openings to be free of shadow effect by the window ledge or the wall above the window. This illustrates how dosimeters should be oriented in high dose-rate gradients to obtain realistic values. The extreme cases illustrating non-agreement have been presented here to emphasize the importance of dosimeter placement.



## TWO-STORY, WOODEN-FRAME HOUSE AREA SPREAD EXPERIMENTS

A second building, a two-story, wooden-frame house, was constructed in model form. The original intention was to model the two-story, wooden-frame house (as described in a previous report<sup>8</sup>) which was tested at the Nevada Test Site. An error was made in the scaling ratios of wall thicknesses, however, and the model was constructed with walls which were too thick. This error was not discovered until fabrication of the model was complete. Since it was late in the year, it was decided to use this model in place of the intended model in order that experiments could be performed before the snow closed down operations at the model facility for the winter. Thus, though the over-all geometry of the scaled two-story house was similar to the two-story, wooden-frame house, direct comparisons of experimental data could not be made.

### 1. Description of the Two-Story House

Though the mass thicknesses of the scale model house were quite different from those of the two-story, wooden-frame house previously tested at Nevada, both structures are described in some detail in this section as their heights and floor plans are nearly identical.

The full-scale building, Figure 26, was a two-story house with a full basement, light-weight walls, shingled roof, and a brick fireplace and chimney at one end. The outside dimensions of the building were 33 feet, 4 inches by 24 feet, 8 inches. Walls were of typical wooden construction with 2- by 4-inch studs on 16-inch centers. The studding was covered on the exterior with approximately 2 inches of wood sheathing and siding, and on the interior with 3/8-inch plywood. First floor and roof joists were 2- by 10-inch timbers on 16-inch centers, while second floor and attic floor joists were of 2- by 8-inch stock of similar spacing. The basement walls were 8 inch-thick poured concrete and contained 7 small windows opening into window wells. An exterior basement door connected to a set of outside concrete steps leading to ground level.

The 1/12-scale steel model of this building, as assembled at the center of a simulated area spread of contamination, is shown in Figure 27. Figure 28 shows

---

<sup>8</sup>J. F. Batter, et al., op. cit.

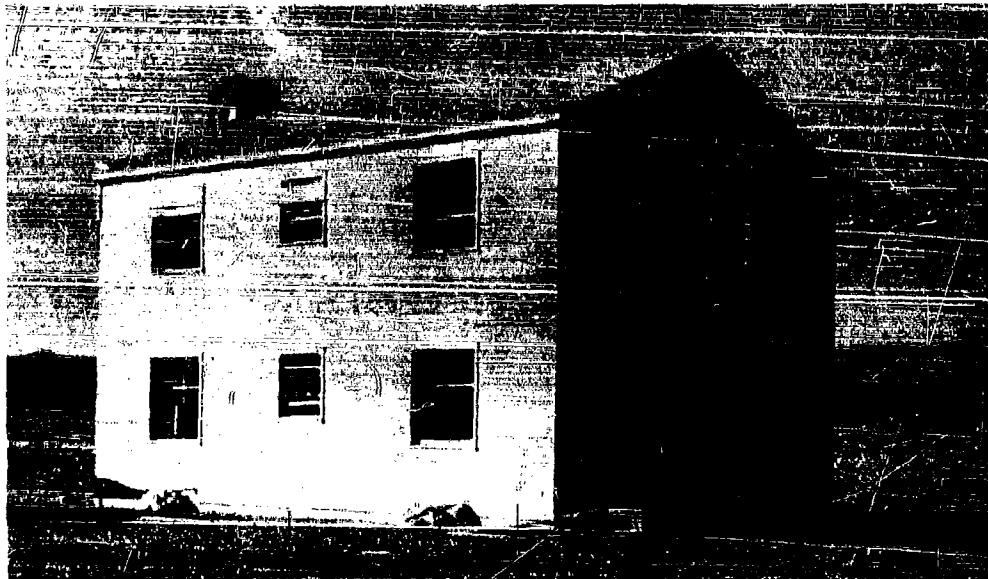


Figure 26. Photograph of Full-Size, Two-Story, Wooden-Frame House

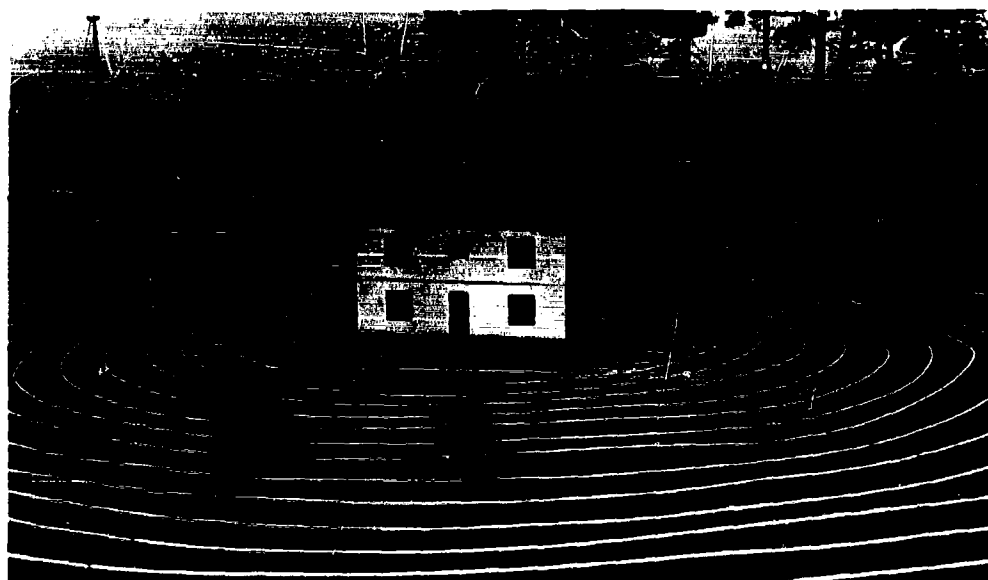


Figure 27. Photograph of Scale Model of Two-Story, Wooden-Frame House

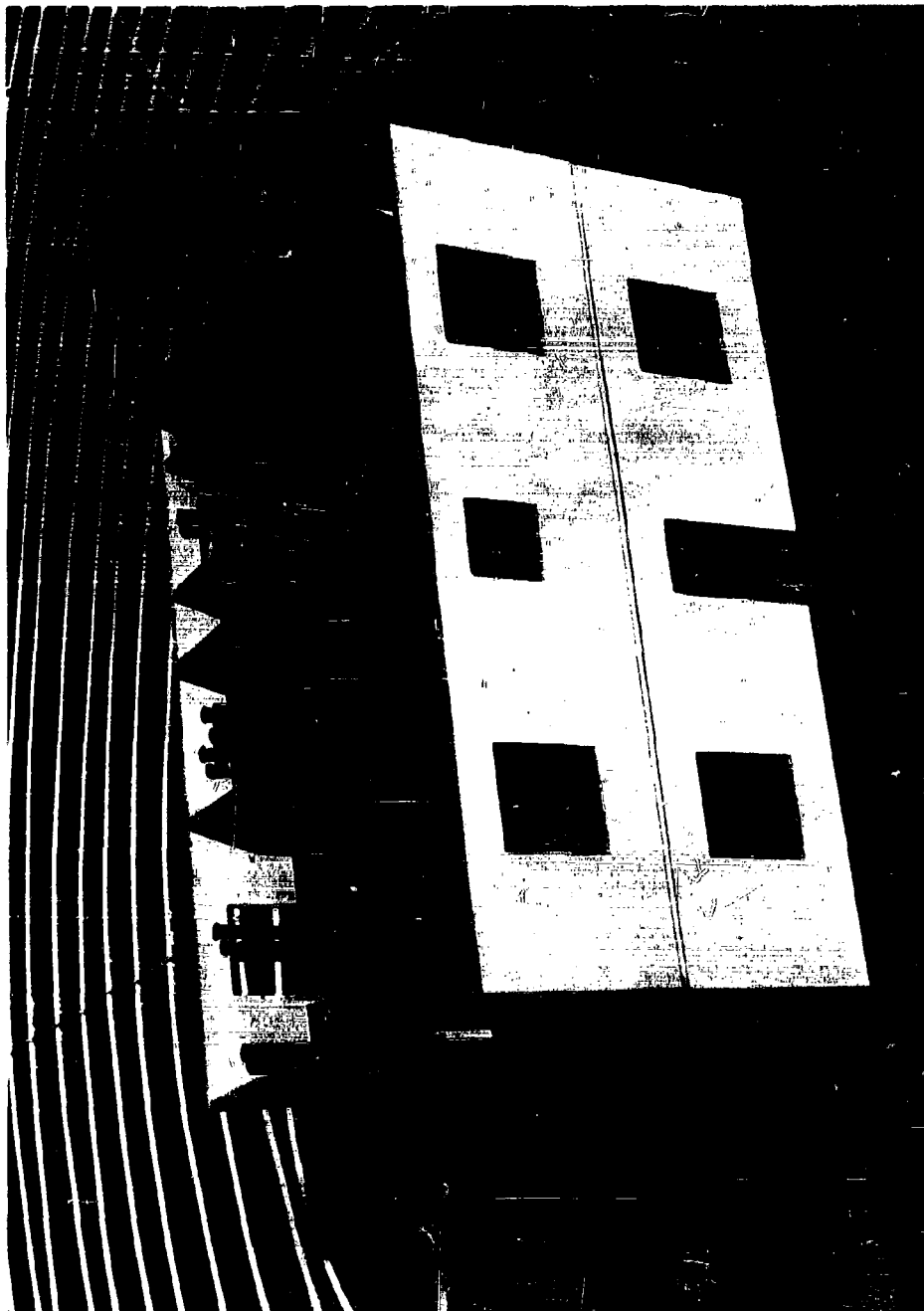


Figure 28. Two-Story Model House Showing Placement of Dosimeters

(1)

the placement of dosimeters in the house. Figures 29 and 30 illustrate the dosimeter placement and construction details of the first and second stories respectively, while Figure 31 illustrates the basement. Figure 32 shows a typical vertical section of the two-story model house. The interior dimensions of the basement were scaled to 1/12 the full-size basement giving 32-1/4 by 23-1/2 inches. A model basement wall thickness of 2-7/16 inches was necessary to duplicate the mass per unit of surface area of the 8 inch-thick concrete walls of the full-size basement. The floor of the basement was made of 1-1/4 inch-thick steel to duplicate mass per unit area of the 3 inch-thick concrete floor. The 8 foot-wide by 11 foot-long by 6-1/2 feet-high OCDM basement shelter existing in the full-size structure was scaled to 1/12 the outside dimensions. The walls and roof of the full-size shelter were of 8 inch-thick solid concrete block, thus also giving an equivalent steel thickness of 2-7/16 inches. The labyrinth-type entrance wall was of the same thickness. One side of the basement stairs was supported by an 8 inch-thick reinforced concrete blast shelter and the other side bounded by an 8 inch-thick concrete load-bearing wall. These, as well as the walls and roof of the blast shelter, are also equivalent to 2-7/16 inches of steel in the model. The outside dimensions of the steel model of this shelter could not be held and still have space left in the shelter for dosimeters. Thus outside dimensions and stair widths were compromised to obtain the required space. The stairs were approximated by using a 1/8 inch-thick steel strip in place of actual stairs.

Mocking up scaled models of shelters in the basements and still maintaining a steel mass per unit area equal to that of the full-size concrete walls can give severe distortion in the ratio of solid-to-air volume between the model and its comparable full-size basement. For the corner basement shelter, this was not too severe, but for the blast shelter, a more dense model material should probably have been used to give a more realistic spacing comparison. Maintaining the inside dimensions of the scaled basement wall assures the most realistic scaling inside the building. The fact that the exterior walls of the model basement extended outside the walls of the first and second stories had no adverse effect in this experiment.

The average solid wood thickness of the walls for the first and second floors of the full scale house is 2-7/8 inches and is equivalent, on a weight per unit area

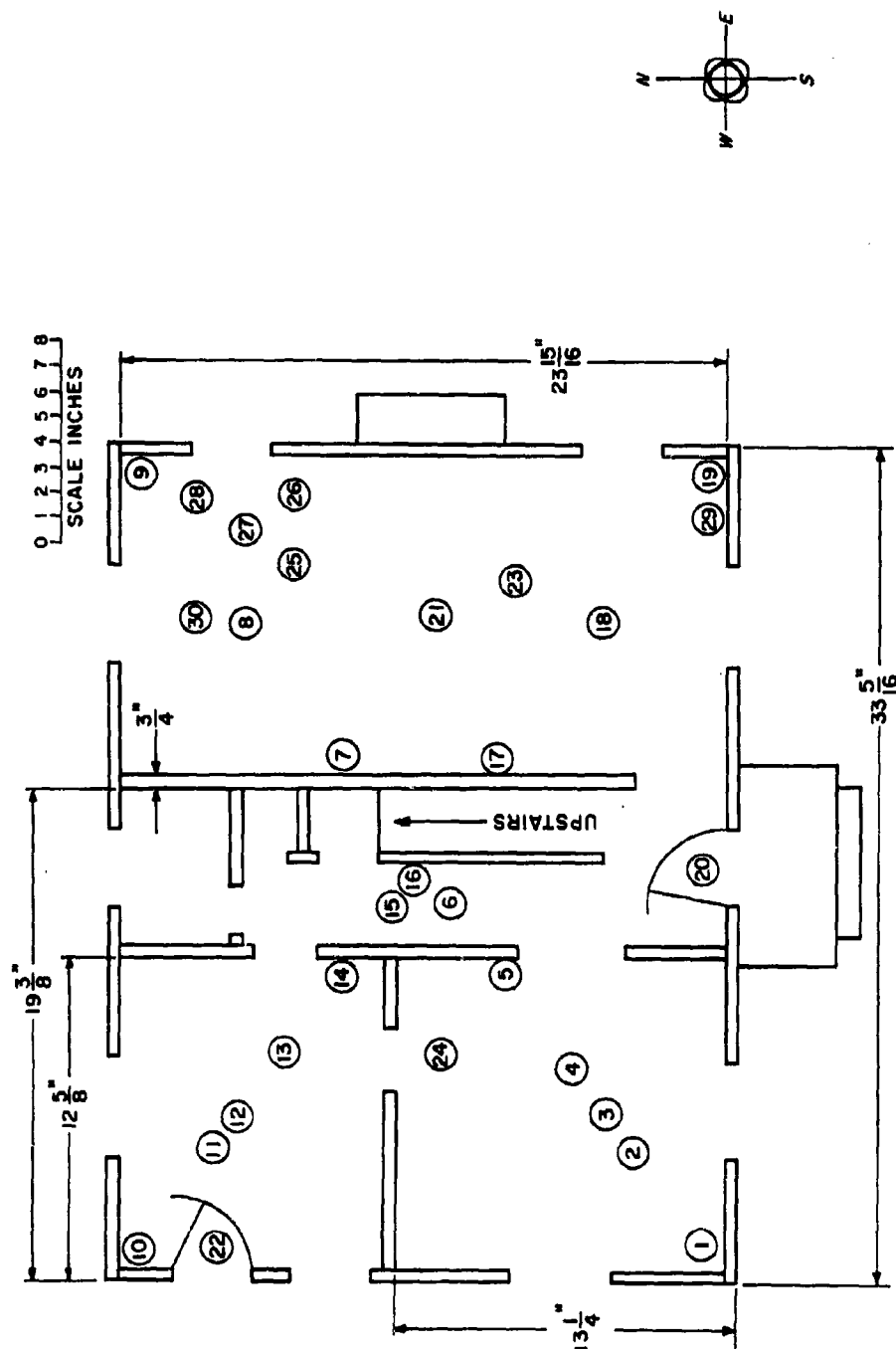


Figure 29. Plan View of First Floor Giving All Dosimeter Locations for Two-Story House

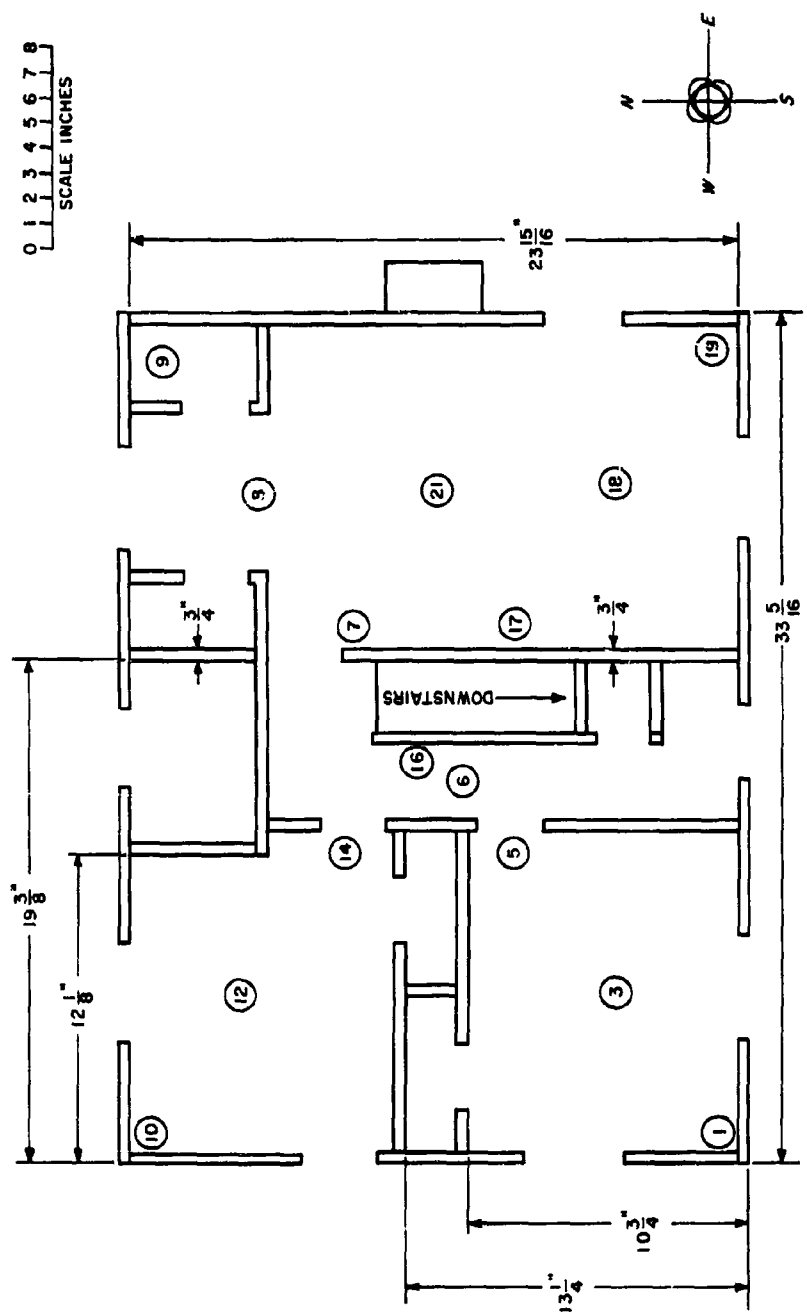


Figure 30. Plan View Giving Dosimeter Positions for the Second Floor of Two-Story Model House

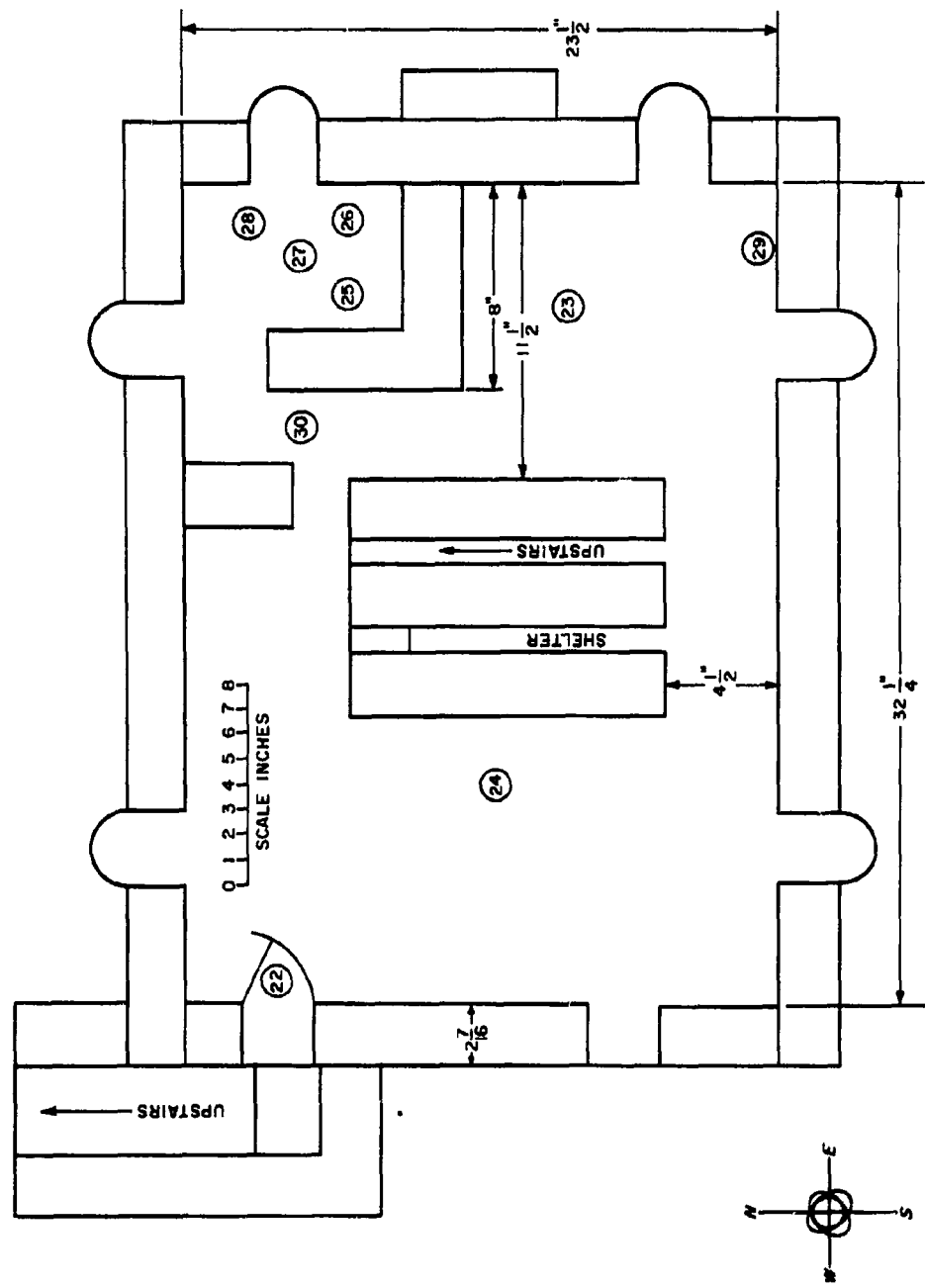


Figure 31. Plan View Giving Dosimeter Positions for the Basement of Two-Story Model House

basis, to  $3/16$  inch ( $7.5 \text{ lb/ft}^2$ ) of steel. The exterior wall thickness of this model house was, however, fabricated of  $3/8$  inch ( $15 \text{ lb/ft}^2$ ) thick steel. This thickness is in error as far as the Nevada two-story, wooden frame house is concerned, but it nearly matches a wall with plastered inside face ( $12 \text{ lb/ft}^2$ ) in place of the  $3/8$  inch-thick plywood. All partitions of the model building may thus be assumed to represent walls plastered on both sides, whereas in the full-scale building the partitions were faced with  $3/8$  inch-thick plywood. The partition weight of the full-size house was approximately  $3 \text{ lb/ft}^2$

which is equivalent to  $0.075$  inch of steel. As noted in a previous report,<sup>9</sup> the combined weight of one wall and one partition for this building is taken as  $8 \text{ lb/ft}^2$  as compared to  $35 \text{ lb/ft}^2$  in the  $1/12$ -scale steel model. The first and second floor, second floor ceiling, and the roof of the full-size house have an average weight of  $7.25$  pounds per square foot, which is equivalent to  $3/16$  inch of steel. The second story floor and ceiling are relatively light weight because of the use of  $3/8$ -inch plywood ceilings in place of plaster.

The model building was fabricated into four separate components. The basement walls and bottom were tack-welded into a single unit. Each basement wall was made up of three matching pieces of steel, each flame-cut to the contour of the wall, including window and door openings. Two

<sup>9</sup> Auxier, Buchanan, Eisenhower, and Menken, op. cit.

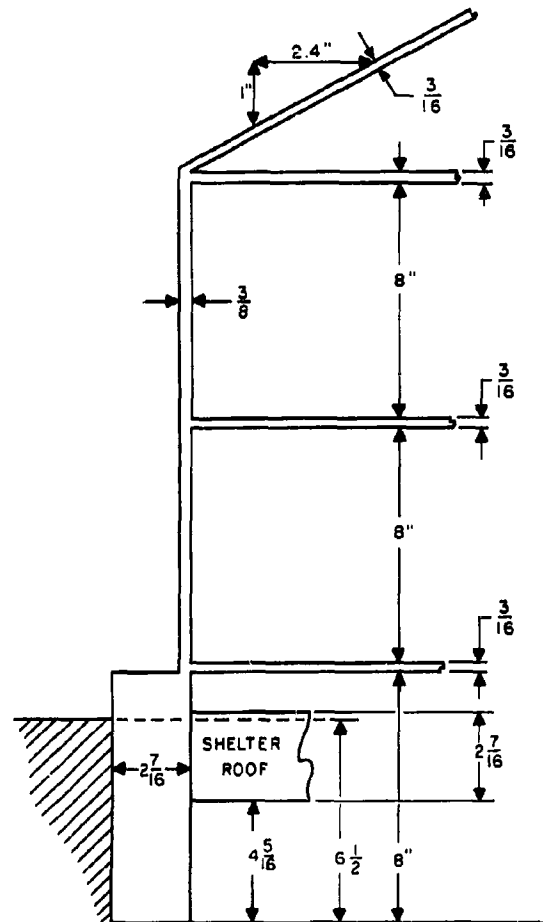


Figure 32. Typical Vertical Section of Two-Story Model House



of the pieces were 1-inch thick and the third 7/16-inch thick giving a combined thickness of 2-7/16 inches. The 1-1/2 inch-thick basement bottom was formed from 1 inch and 1/2 inch-thick plates. The first and second stories were each tack-welded into separate units. The walls of each story were flame-cut to shape, including doors and windows. The four wall pieces, each 3/8-inch thick and 8-inches wide, plus a 3/16 inch-thick floor sheet, were welded into a unit. Partitions were cut to size from 1/2 inch-thick plates and taped into position. The fourth and final unit consisted of the roof and second floor ceiling, plus the two 3/8 inch-thick attic end walls. The model was assembled by setting one unit on top of another in proper order.

## 2. Experimental Procedures

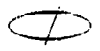
The model house was positioned in the center pit of the radiation facility with the basement recessed below ground level in the same manner as the full-size basement. Concrete blocks were used to fill the remaining pit volume to ground level. Basement windows were left covered with concrete block, since window wells of the full-size building had been sandbagged.

Measurements of the gamma-ray dose (cobalt-60) rate in the two-story model were made by using a simulated radiation field of 45-foot radius on the ground with no roof contamination. Because of a general lack of symmetry in the interior portions of the model, it was necessary to provide a full 360-degree area spread with the experimental building in the center. The dose rate was measured at several heights at a total of forty positions within the structure using 2r Landsverk dosimeters. An area spread of fallout contamination was simulated by pumping a 10-curie, cobalt-60 source through 4600 feet of polyethylene tubing in a manner such that the product of source speed and the area per linear foot of tubing remained constant.

The first loop of tubing around the model building followed its rectangular contour at an average distance of 2 inches from the basement wall. The tubing then spiraled outward with 6-inch spacing to a 10-foot radius from the center of the building. The beginning rectangular contour was gradually softened into a circular shape with succeeding tubing loops.

(7)

In mocking up a uniform fallout field where radioactive contaminants are spread evenly over the ground, it is necessary to control source positions so that the aggregate radiation received by the experimental house and its instrumentation will be essentially identical to that received from a uniform field. When pumping the source at a controlled rate through prepositioned tubing, the activity per unit length of tube represents the activity of an area equal to the tube spacing times the unit tube length. With a 6-inch spacing, the source density per inch of tube represents the source density of 6 square inches of area spread. As the spacing approaches zero, the ideal uniform field is also approached, except for undesirable shielding by the tubing and its contained fluid. Close spacing increases the tubing lengths which in turn complicate the job of arranging the tubing into an area spread. For the experimental run on the two-story, wooden-frame house, the source tubing was spaced as tightly as practical without unduly increasing the tubing length required for a 90-foot diameter area spread. A compromise spacing of 6 inches was set for the model house experiments and extended out to a radius of 10 feet. Even with spacing as close as 6 inches, instrumentation in the experimental building will, in effect, view a few of the innermost loops as distinct loops with finite space between them. Loops only a short distance from the house will appear as part of a uniform area of tubing without space between loops. The error in dosimeter measurements introduced by the first few loops not appearing as a perfect fallout field will, however, be small as compared to the dose rate from the entire area spread. Continuing the 6-inch spacing beyond a 10-foot radius served no useful purpose in maintaining an effectively uniform area spread as long as spacing was not increased enough to appear at the house as other than a solid tubing area. Maintaining the 6-inch spacing beyond a 10-foot radius would require the use of 12,000 feet of tubing for a 90 foot-diameter area spread. The spacing was arbitrarily increased to 1 foot between a 10 and 25-foot radius and again increased to 2 feet between 25 and 45 feet. The tube length in the inner annulus was 680 feet, 1770 feet in the middle annulus, and 2040 feet in the outer annulus. To maintain a constant source density with these spacings, it is necessary to make the source speed in the 12-inch spacing at  $1/2$  and in the 24-inch spacing at  $1/4$  the source speed in the 6-inch spacing area. Source velocity is governed directly by pump flow rate. Thus the product of source speed times area simulated per linear foot of tubing was maintained at a constant value by varying



the pump (and hence source) speed inversely as the spacing of the tubing. Sixty feet of tube length was allowed on each end of the area spread tubing for connection with a source container located outside of the area spread.

The source was always pumped through the area spread from its outer edge to the center. By observation of the source through a 20-power spotting scope located on a hillside overlooking the test facility, timing could be coordinated for changing pump speed and the resulting source velocity as tube spacing changed. Also, at the moment the source completed the area spread, the high-output gear pump was cut in to push the source rapidly from the center of the area spread to the source storage container. For auxiliary runs to improve the match of dosimeter readings to the wide range of dose experienced in various parts of the building, the area spread was broken into two sections. The first contained the tubing with the 6-inch spacing and, the second, the tubing with 12- and 24-inch spacings. The tubing at the junction of the 6- and 12-inch tubings was cut and tube fittings attached so that either of the two sections could be used separately or in series.

Experimental operating procedures were the same as for the ring experiments on the precast concrete house, except for the variations in source position programming just discussed and the omission of lead bag shielding of the leads to and from the area spread. The 4600 feet of tubing were laid down on the facility pad in the pattern previously described. The tubing was attached to the hot topping with conduit nails at 45-degree intervals to prevent the tubing from being moved by the wind and by rain water. Lead connections were the same as for the precast concrete house experiments. A 1000-pound capacity, gantry-type "A" frame with hoist was used to lift the model house off its basement for the placement and removal of dosimeters in the basement. Dosimeters were placed and removed from the first and second floor of the model house through door and window openings. Three types of dosimeters were used: 10-mr, 200-mr Victoreen, and 2r Landsverk (L-81) pocket ionization chambers.

### 3. Measurements and Results

Three experimental runs were made on the two-story model house to determine gamma-radiation attenuation within upper floors of the building, basement, and basement fallout shelter.

(1)

The first experiment was a check on the exposure within the building by the source while traversing the entire 4600 feet of polyethylene tubing to make certain that dosimeter readings would fall between 20 and 80 per cent of their full range. For the check run, a dozen dosimeters were placed at positions of anticipated extreme dose rates within the first and second floor of the model. The source was then pumped through the tubing at rates estimated to give optimum dosimeter readings. As a result of this run, it was determined that the total exposure time should be about 3-3/4 hours.

The second experimental run measured dose rates along horizontal diagonal traverses for both the first and second floor. One hundred and four 2r dosimeters were placed at the positions shown in Figures 29, 30, and 31 at heights of 2-1/2, 5-1/2, 8-1/2, 10-1/2, 13-1/2, and 16-1/2 inches above ground level and 1, 4, and 7 inches above floor level. Additionally, one 2r dosimeter was placed at the basement outside exit and 5 200-mr dosimeters were placed near the center of the basement. Four of the 200-mr dosimeters were mounted horizontally—2 at floor level and 2 at ceiling level—at positions 23 and 24. The fifth 200-mr dosimeter was mounted vertically at position 24 to integrate the dose rate between the basement and ceiling. A 10-mr dosimeter was placed in the basement fallout shelter. The 10-curie, cobalt-60 source was then pumped through the three connected tubing annuli, at the source speeds determined from the check run. Control of the source through the three annuli was excellent. The source uniformly traversed the outer annulus in 145 min, 0 sec, the middle annulus in 67 min, 3 sec, and the inner annulus in 13 min, 3 sec for a total exposure time of 3 hours, 45 minutes, and six seconds. Normalized dose rates in the building due to this area spread exposure are given in Tables VI and VII. The 2r dosimeter readings in the first and second stories of the model ranged from 30 to 80 per cent of full-scale dose and were therefore within their most accurate range. The same applied to the 200-mr dosimeters in the center of the basement. The 10-mr dosimeter in the shelter, however, was completely discharged.

The third experimental run on the two-story, wooden-frame house was performed to obtain dose-rate values in the basement corner fallout shelter and to check dose rates in the central area of the basement. Eight 10-mr dosimeters were placed

horizontally within the fallout shelter at 3-1/2 and 5-1/2 inches below ground level as shown in Figure 31. Three 200-mr dosimeters were horizontally mounted at position 23 for a comparison check of the dose rate between this and the previous run at the center region of the basement. Three additional dosimeters were placed horizontally at position 29 to obtain dose-rate values in a corner of the basement. These dosimeters were 1, 3-1/2, and 6 inches below ground level.

In order to obtain dose readings within the capacity of the 10-mr dosimeters used in the basement shelter, it was necessary that the area spread be divided into 2 separate sections, so that the source could be pumped through each section independently of the order. This necessity was illustrated in the second experiment when the shelter dosimeter went full-scale during a minimum exposure for a 4600-foot continuous-tube length. The inner annulus contained the 680 feet of tubing, had a tube spacing of 6 inches, and an outer diameter of 21 feet. This section was calculated to contribute 56.5 per cent of the dose rate at the center of a cleared circle of area equivalent to that occupied by the model test building. The second tube section consisted of the remainder of the 90 foot-diameter area spread. By running the source through each section independently of the other, the accumulated dose within the basement shelter from the area spread could be broken into two values; one for each section. Each value would be approximately 1/2 the total area spread dose and should fall within the dose range of the 10-mr dosimeters used in the basement shelter. A complete area spread experiment could then be made on the building by using 2r dosimeters in the first and second stories of the model, 200-mr dosimeters in the open basement area, and 10-mr dosimeters in the basement shelter. The 2r and 200-mr dosimeters would be read only at the end of the exposure from both tubing sections. The 10-mr dosimeters would be read (and automatically recharged) at the end of the exposure by each area spread section. The combined components for each of the 2 sections on the 10-mr dosimeters gave the total area spread dose in the shelter.

For the third experiment, the source was pumped through the inner section of the area spread in 12 minutes and 52 seconds. Source velocity was the same as that used in the complete area spread (4600 feet) experiment previously described. The model building was then lifted from its basement and the basement dosimeters

TABLE VI

## DOSE RATE DATA FOR TWO-STORY MODEL HOUSE

(90 Foot-Diameter Source Field, Cleared-Roof Data Normalized  
to Infinite Field Value of 1 r/hr at 1 Meter Height—Source Density:  
0.024 curie/meter<sup>2</sup>—Values in mr/hr)

Position No.*	Dosimeter Height (Inches from Ground)								
	1 $\frac{1}{2}$	2 $\frac{1}{2}$	5 $\frac{1}{2}$	8 $\frac{1}{2}$	9 $\frac{1}{2}$	10 $\frac{1}{2}$	13 $\frac{1}{2}$	16 $\frac{1}{2}$	17 $\frac{1}{2}$
1	FIRST FLOOR	452V	497V	497V	SECOND FLOOR	357H	394H	359H	CEILING, SECOND FLOOR
2		368V	465V	420V					
3						302H	352H	352H	
4		300V	386V	340V					
5		276V	326V	402V		198H	251H	311H	
6		193V	296V	267V		193H	255H	235H	
7		255V	285V	216V		204H	225H	276H	
8		306V	435V	418V		272H	321H	358H	
9		445V	520V	493V		308H	326H	313H	
10		352H	474H	432H		410V	427V	368V	
11		317H	202H	188H					
12						386V	386V	386V	
13		313H	343H	382H					
14		193H	294H	367H		248V	335V	244V	
15		221H	286H	313H					
16						225V	230V	250V	
17		239H	300H	313H		260V	310V	294V	
18		194H	378H	378H		342V		306V	
19		565H	500H	454H		377V	414V	342V	
20			470H						
21		250H		342H		248H		362H	
21		328H <sup>1</sup>	360H <sup>2</sup>			313H <sup>3</sup>	294H <sup>4</sup>		

\* See Figure 29

H = Horizontal Dosimeter

V = Vertical Dosimeter

<sup>1</sup>Height: 4-1/2 inches<sup>2</sup>Height: 6-1/2 inches<sup>3</sup>Height: 12-1/2 inches<sup>4</sup>Height: 14-1/2 inches

TABLE VII  
DOSE RATE DATA FOR BASEMENT OF TWO-STORY MODEL HOUSE  
(Cleared-Roof Data Normalized to Infinite Field Value of 1 r/hr at  
1 Meter Height—Source Density: 0.024 curie/meter<sup>2</sup>—Values in mr/hr)

Position No. *	Dosimeter Height (Inches from Ground)					
	-6	-5 $\frac{1}{2}$	-3 $\frac{1}{2}$	-2 $\frac{1}{2}$	-1	+1
90 Foot-Diameter Area Spread						
22		53V	62V		76V	
23	21H					71H
24	26H			48V		77H
27		0. S.				
21.2 Foot-Diameter Area Spread						
23	12H		20H		33H	
25		3.3H	3.2H			
26		3.5H	0. S.			
27		0. S.	0. S.			
28		0. S.	0. S.			
29	7H		12H		45H	
30			10V			

\* See Figure 29

H = Horizontal Dosimeters  
V = Vertical Dosimeters  
0. S = Off Scale

read on the charger-readers. Unfortunately, because of the sudden arrival of severe snow and ice conditions, this run, plus plans for more thorough basement studies, were brought to an abrupt halt. Measurements (taken in the basement) of exposures from the inner section of tubing only were normalized, however, and are given in Table VII.

#### 4. Discussion of Model Results

As mentioned previously, the model house did not simulate the wall thickness of the two-story, wooden-frame house as constructed in Nevada, except in the basement area. Thus, direct comparison of model experimental data with that obtained from a full-scale structure was not possible. In order to evaluate the experimental results obtained from the model house, it was decided to compute the shelter factors

(1)

obtainable from a full-size house with geometry and wall thicknesses similar to the model, and compare these results to those obtained experimentally from the model. This was done in the following manner:

First, selecting a position within the house, the structure around the location was idealized into one or more "ideal houses" for ease of computation. For example, consider position 8 (Figure 29) on the first floor. The total dosage arriving at position 8 was assumed to be equal to one half the dose that would be obtained at the center of a 12- by 13-foot house with 3/8 inch-thick iron walls containing 1 window per wall (representing the radiation received from the sector from northwest to southeast), plus 1/4 the dosage received from a house with dimensions of 13 by 36 feet with walls of 3/8 inch-thick steel (representing dosage received from the southeast to southwest sector), plus 1/4 the dose received from a house of 36- by 52-foot dimensions with walls of  $3/4 + 1/2 + 3/8$  inch =  $1-5/8$  inches of iron.

Next the wall thicknesses were converted to equivalent electron thicknesses of water and expressed as pounds per square foot. (This was necessary so that the OCDM shelter penetration tables could be used.) This data was then used as entries to the tables in the OCDM's "Guide for Fallout Shelter Surveys" (April, 1959) to compute the dose rates at 3 foot heights that would be obtained from an infinite ground field, with a cleared circle. The computation of the variation of dose rate with height was performed using Spencer's results.<sup>10</sup> An additional correction was made for the dosimeter positions near the floor on the second floor, 2 or more feet from the outer walls to allow for the fact that much of the radiation reaching these locations had to penetrate the ceiling of the first floor.

Protection factors from ground radiation were then calculated by dividing the normalized dose rate at 1 meter (3 r/hr) by the dose rate determined from the above analysis. Table VIII presents this data together with that obtained from the experiments on the model house for comparison purposes. The protection factors for the model were obtained by dividing the calculated dose rate from a source configuration

---

<sup>10</sup>L. V. Spencer, "Structure Shielding against Fallout Radiation from Nuclear Weapons," OCDM, to be published.



TABLE VIII

TWO-STORY MODEL HOUSE PROTECTION FACTORS COMPARED TO  
FULL-SCALE HOUSE OF SAME WALL THICKNESSES<sup>†</sup>

(Protection Factors Presented as Experimental/Analytical)

Position No.**	Dosimeter Height (Inches from Ground)								
	1 1/2	2 1/2	5 1/2	8 1/2	9 1/2	10 1/2	13 1/2	16 1/2	17 1/2
1	FIRST FLOOR	1.7/1.7	1.5/1.9	1.5/2.0	SECOND FLOOR	2.2/2.1	2.0/2.3	2.1/2.4	CEILING, SECOND FLOOR
2		2.0/1.7	1.6/1.9	1.7/2.0		----	----	----	
3		----	----	----		2.4/2.5	2.0/2.4	2.0/2.5	
4		2.3/2.0	1.8/2.2	2.0/2.4		----	----	----	
5		2.5/2.5	2.1/2.7	1.7/2.9*		3.4/3.5	2.7/3.3	2.2/3.5*	
6		3.5/2.5	2.3/2.8	2.5/3.0		3.5/3.6	2.6/3.4*	2.9/3.6	
7		2.7/2.3	2.4/2.5	3.1/2.7*		3.3/3.1	3.0/3.0	2.5/3.2	
8		2.3/1.7*	1.8/1.9	1.7/2.0		2.6/2.3*	2.2/2.2	2.0/2.3	
9		1.7/1.7	1.5/1.9	1.8/2.0		2.5/2.1*	2.4/2.3	2.4/2.4	
10		2.2/1.7*	1.6/1.9	1.8/2.0		1.9/2.1	1.8/2.3	2.1/2.4	
11		2.3/1.7*	3.6/1.9*	3.8/2.0*		----	----	----	
12		----	----	----		1.9/2.3	1.9/2.3	1.9/2.4	
13	FIRST FLOOR	2.2/2.0*	2.0/2.2	1.8/2.4	SECOND FLOOR	----	----	----	CEILING, SECOND FLOOR
14		3.5/2.5*	2.3/2.7	2.6/2.9		2.7/3.5	2.0/3.3*	2.3/3.5	
15		3.0/2.5*	2.4/2.8	2.2/3.0		----	----	----	
16		----	----	----		3.0/3.6	2.9/3.4	2.7/3.6*	
17		2.8/3.0	1.9/2.5	2.2/2.7		2.6/3.1	2.2/3.0	2.3/3.2	
18		3.7/1.7*	1.9/1.9	1.9/2.0		2.1/2.3	----	2.3/2.3	
19		1.4/1.7	1.5/1.9	1.7/2.0		2.0/2.1	1.9/2.3	2.2/2.4	
20		----	1.5/1.6	----		----	----	----	
21		2.8/1.8*	----	2.0/2.1		2.8/2.5	----	1.9/2.5	
21		2.1 <sup>(1)</sup> /1.9	1.9 <sup>(2)</sup> /2.0	----		2.2 <sup>(3)</sup> /2.4	2.4 <sup>(4)</sup> /2.4	----	

\* Ratio of calculated to experimental protection factor greater of less than 1.15 ± 20%.

\*\* See Figure 29

<sup>(1)</sup> Height: 4-1/2 inches<sup>(2)</sup> Height: 8-1/2 inches<sup>(3)</sup> Height: 12-1/2 inches<sup>(4)</sup> Height: 14-1/2 inches<sup>†</sup> Calculated according to method outlined in "Guide for Fallout Shelter Surveys," Preliminary Edition, OCDM, April (1959).

(1)

identical to that used in the model experiment, at 1/12 meter height above the ground, by the dose rate obtained from the model experiments. The dose rate at any position above the cleared circle was calculated as described in Appendix B.

#### 4.1 Upper Floors of Two-Story House

Part of the calculated and experimental protection factors given in Table VIII are presented as vertical and horizontal traverses of the model building in Figures 33 through 36. Figure 33 shows a vertical traverse at the center of the building and Figure 34 at the center of the living room and second floor directly above it. Figures 35 and 36 present horizontal traverses 4 inches above the first and the second-story floors respectively.

An analysis of the calculated and experimental protection factors of Table VIII shows that agreement was very good. The average ratio of the calculated protection factors to the experimental protection factors was found to be 1.15. In other words, the calculated protection factors were 15 per cent higher than those determined experimentally. It was also interesting to note that the distribution of the individual position values was such that 81 per cent of the positions were within  $\pm 20$  per cent of the 1.15 factor and 59 per cent within  $\pm 10$  per cent. It can be further shown that a factor of approximately 1.15 is to be expected between calculated and experimental values. The calculated values of the protection factor were based upon penetration curves presented in an OCDM report.<sup>11</sup> These curves are predicated upon a 1.12 hour-fallout radiation penetration of water barriers. As previously mentioned, the calculations of the protection factors were based upon a conversion of iron walls to water walls of equivalent electron density and the attenuation curves in the OCDM report<sup>12</sup> were used. The ratio of calculated protection factors to experimental protection factors was found to be about 1.15. This result is to be expected, since the ratio of cobalt-60 to the 1.12 hour-fallout spectrum attenuation in water is 1.06 to 1.13<sup>13</sup> for mass thickness of 20 to 100 lbs/ft<sup>2</sup>, and since skyshine is not properly simulated in the model. The walls of the model building varied from 13 to 80 lbs/ft<sup>2</sup>.

<sup>11</sup>"Guide for Fallout Shelter Surveys," Preliminary Edition, OCDM, April (1959).

<sup>12</sup>Ibid.

<sup>13</sup>L.V. Spencer, op. cit., Figure 26.6.

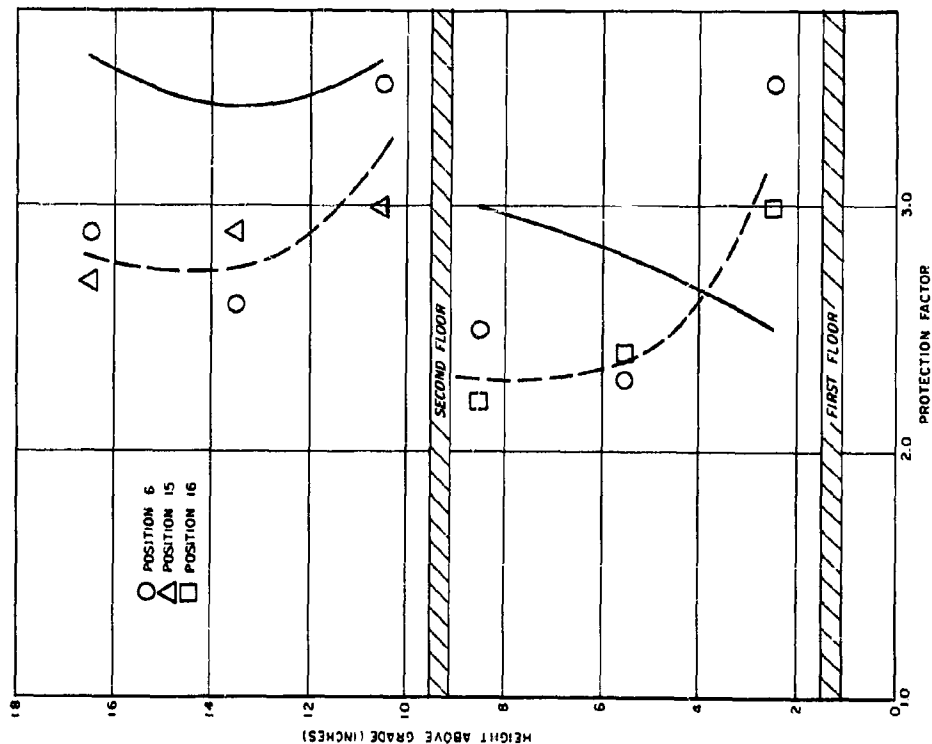


Figure 33. Vertical Plot of Protection Factors at Center of Two-Story Model House

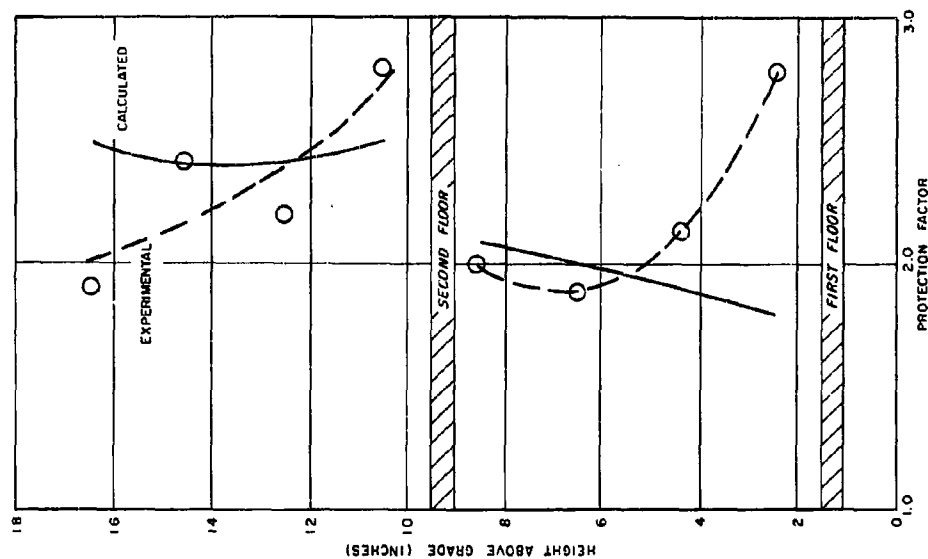


Figure 34. Vertical Plot of Protection Factors at Center of Living Room in Two-Story Model House

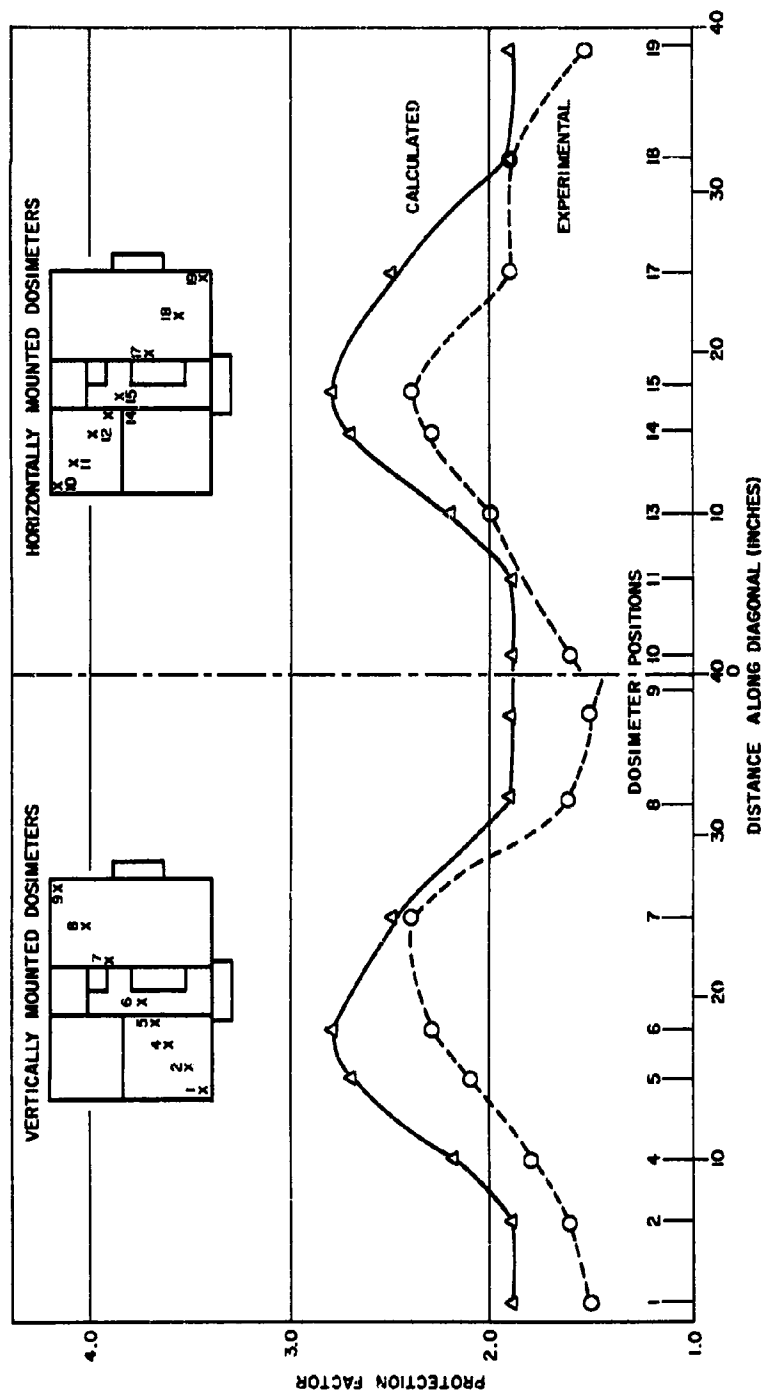


Figure 35. Protection Factors for First Floor of Two-Story Model House

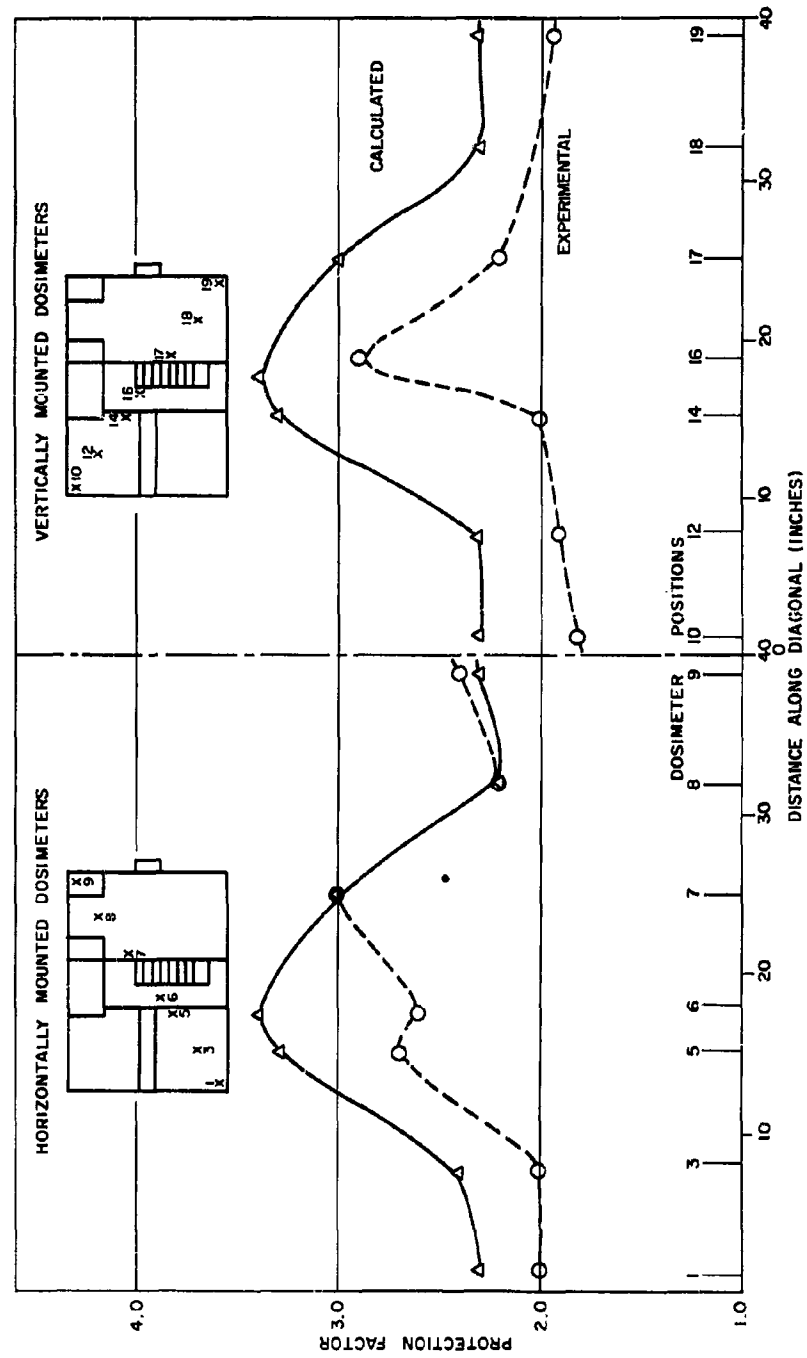


Figure 36. Protection Factors for Second Floor of Two-Story Model House

(1)

It is important to note that approximately one-half of the positions in Table VIII, having values beyond  $\pm 20$  per cent of the 1.15 ratio of the calculated-to-experimental protection factor, are located in the lowest elevation on the first floor. The majority of these values are such that the measured protection factors are greater than would be expected from calculated results. This may be attributed to additional attenuation of gamma rays penetrating the lip of the model basement which extended above ground level (see Figure 32). This penetration was not considered in the computed protection factors. Of the remaining positions with a greater than  $1.15 \pm 20$  per cent ratio, the cause in many instances may be attributed to local variations due to door and window openings which allowed gamma rays (particularly from the close-in field) to impinge directly on a dosimeter. Gamma rays passing through openings and one wall or ceiling will have the same effect, but to a lesser degree.

#### 4.2 Basement of Two-Story House

Though few experimental measurements were obtained for the basement of the model two-story house, it is desirable to compare them with readings obtained from experimentation upon the two-story, wooden-frame house at Nevada, as the geometry and mass thicknesses of the basement portion of both structures are nearly identical. Table IX (and a previous report<sup>14</sup>) presents the results of experimentation with source rings on the two-story, wooden-frame house normalized to a source strength of one curie per foot of circumference.

To compute the dose rates that would be obtained in the basement of the two-story, wooden-frame house from an annular ground field of contamination with a cleared roof, the following procedure is used.

The dose rate at any position in the basement should be proportional to the direct flux in the structure above it, as a basement position can only see radiation scattered by the structure above it and the surrounding atmosphere. The direct

---

<sup>14</sup>Clarke, Batter, and Kaplan, op. cit.

TABLE IX

DOSE RATES OF BASEMENT IN TWO-STORY, WOODEN-FRAME HOUSE<sup>†</sup>  
(Data Normalized to 1 curie/ft of Ring Circumference)

Height below Ground Level (feet)	Ring Radius (feet)	Stations						
		22	23	24	25	26	29	30
6	21.2	--	--	--	--	--	71	42
	25.4	--	--	--	17	--	52	43
	31.8	--	--	--	12	10	45	37
	42.4	--	--	--	--	--	31	22
	63.7	--	--	--	--	--	22	--
3	21.2	--	160*	--	19	15	106	--
	25.4	--	140*	--	16	13	79	65
	31.8	--	100*	--	16	--	60	60
	42.4	--	76*	--	--	6	46	38
	63.7	--	62*	--	--	--	32	31
1	21.2	--	290**	--	23	25	--	225
	25.4	--	270**	--	21	--	215	160
	31.8	--	210**	--	--	16	130	110
	42.4	--	130**	--	11	12	93	80
	63.7	--	110**	--	8	--	72	60

\* Height: 3-1/2 ft

\*\* Height: 1/2 ft

† Clarke, Batter, and Kaplan, op. cit.

flux from a source ring of radius  $r$  containing 1 curie of cobalt-60 per foot of circumference may be calculated to be:

$$I_d = \frac{\sigma 2 \pi r B e^{-\mu r}}{r^2} \approx \frac{90,000}{r} \text{ mr/hour} \quad (1)$$

if the point to point buildup factor for cobalt-60 of  $B = 1 + 0.55 \mu r$  is used. Then the ratio of flux scattered into the basement to direct flux may be written as:

$$\frac{I_s}{I_d} = \frac{I_r}{90,000} \quad (2)$$

where  $I$  is the observed value in the basement of the two-story, wooden-frame house, and  $r$  the radius of the source ring. These ratios for positions of interest are shown in Table X where it can be seen that they are nearly independent of ring radius, though they vary with position and detector height as would be expected.

TABLE X  
RATIO OF SCATTERED DOSE IN THE BASEMENT OF TWO-STORY,  
WOODEN-FRAME HOUSE TO DIRECT DOSE ABOVE INFINITE PLANE †

$$\frac{I_s}{I_d} = \frac{Ir}{90,000}$$

Height below Ground Level (feet)	Source Radius (feet)	Stations						
		22	23	24	25	26	29	30
6	21.2	--	-----	--	-----	-----	0.0187	0.0099
	25.4	--	-----	--	0.0048	-----	0.0147	0.0122
	31.8	--	-----	--	0.0042	0.0035	0.0159	0.0119
	42.4	--	-----	--	-----	-----	0.0145	0.0103
	63.7	--	-----	--	-----	-----	0.0155	-----
	Ave. Value	--	-----	--	0.0045	0.0035	0.0155	0.0111
3	21.2	--	0.0380*	--	0.0045	0.0036	0.0249	-----
	25.4	--	0.0396*	--	0.0046	0.0037	0.0222	0.0183
	31.8	--	0.0354*	--	0.0057	-----	0.0211	0.0211
	42.4	--	0.0358*	--	-----	0.0028	0.0217	0.0179
	63.7	--	0.0440*	--	-----	-----	0.0227	0.0220
	Ave. Value	--	0.0366*	--	0.0049	0.0037	0.0225	0.0198
1	21.2	--	0.0685**	--	0.0054	0.0059	-----	0.0530
	25.4	--	0.0760**	--	0.0048	-----	0.0608	0.0450
	31.8	--	0.0745**	--	-----	0.0057	0.0457	0.0388
	42.4	--	0.0610**	--	0.0052	0.0057	0.0438	0.0378
	63.7	--	0.0777**	--	0.0057	-----	0.0510	0.0424
	Ave. Value	--	0.0715**	--	0.0053	0.0058	0.0504	0.0434

\* Height: 3-1/2 ft

\*\* Height: 1/2 ft

† Clarke, Batter, and Kaplan, op. cit.



In order that the dose rate from an annular ground source may be computed, the ratio of direct flux from an annular ground source surrounding the building to that from an infinite field must be calculated. This ratio may be obtained with sufficient accuracy from the appropriate integrals of point-to-point transmission, using a buildup factor of  $B(x) = 1 + 0.55 \mu x$ . Thus:

$$\frac{I_d}{I} = \frac{E_1(\mu\rho) - E_1(\mu\Psi) + 0.55 e^{-\mu\rho} - 0.55 e^{-\mu\Psi}}{E_1(\mu h) + 0.55 e^{-\mu h}} \quad (3)$$

where

- $h$  = Standard height above infinite field = 1 meter
- $\rho$  = Effective radius of cloud roof  $\cong 4.9$  meters
- $\Psi$  = Inner radius of source annulus of interest
- $\mu$  = Total linear absorption coefficient for cobalt gamma rays in air =  $0.00625 \text{ meters}^{-1}$  for Nevada conditions.

Thus for the particular building area and source annuli of interest (78 and 330 meters, outside diameter), the direct radiation would be 0.40 and 0.59 of the values for infinite field. The values shown in Table X must then be multiplied by 0.40 and 0.59 to obtain the dose rates expected from an annular field with radii of 39 and 165 meters, respectively.

Table XI presents both the experimental model data and that obtained from the full-scale, two-story, wooden-frame house using the above technique. Though the absolute agreement is poor, it is of interest to note that the dose rates obtained in the model house are all (except for a few ratios based upon very low dose rates) a factor of about 1.5 - 2.0 higher than those obtained in the full-scale structure. This factor of 1.5 - 2.0 is probably attributable to three major causes:

1. The actual dose readings in the basement of the full-scale house were very low, and hence may have contained considerable error.
2. There was less mass above the basement from which radiation could scatter. Consider the case where there is no mass above the basement. In the absence of an atmosphere there would be no material from which gamma rays might scatter into the basement. The model house faithfully represented the mass thicknesses of the full-scale house in the basement and the floors. However, the interior

TABLE XI  
COMPARISON OF DOSE RATE IN BASEMENT OF TWO-STORY,  
WOODEN-FRAME HOUSE TO THAT OF TWO-STORY MODEL HOUSE  
(mr/hour)

Position	Model/Full-Scale Ratio	Height below Ground Level (feet)						
		-6	-5½	-3½	-3	-2½	-1	+½
90 Foot-Diameter Model Source Annulus								
22	Model	-----	53	62	---	--	76	-----
	2-Story, Wooden- Frame	-----	-----	-----	---	---	---	-----
	Ratio	-----	-----	-----	---	---	---	-----
23	Model	21	-----	-----	---	---	---	71
	2-Story, Wooden- Frame	10.5*	-----	21	---	---	42	71*
	Ratio	2.0	-----	-----	---	---	---	1.0
24	Model	26	-----	-----	---	48	---	77
	2-Story, Wooden- Frame	-----	-----	-----	---	---	---	-----
	Ratio	-----	-----	-----	---	---	---	-----
21.2 Foot-Diameter Model Source Annulus								
23	Model	12	----	20	---	--	33	-----
	2-Story, Wooden Frame	7*	----	14.7	---	--	30	-----
	Ratio	1.71	----	1.36	---	--	1.10	-----
25	Model	-----	3.3	3.2	---	--	---	-----
	2-Story, Wooden- Frame	1.8	1.85*	1.95*	2.0	--	2.1	-----
	Ratio	-----	1.78	1.64	---	--	---	-----
26	Model	-----	3.5	-----	---	--	---	-----
	2-Story, Wooden- Frame	1.4	1.43*	-----	1.5	--	2.3	-----
	Ratio	-----	2.45	-----	---	--	---	-----
29	Model	7.0	----	12	---	--	45	-----
	2-Story, Wooden- Frame	6.2	----	8.0*	9.0	--	20	-----
	Ratio	1.13	----	1.5	---	--	2.25	-----
30	Model	-----	-----	10	---	--	---	-----
	2-Story, Wooden- Frame	4.5	-----	6.7*	7.9	--	17	-----
	Ratio	-----	-----	1.49	---	--	---	-----

\*Values obtained from plot of vertical traverses.

and exterior partitions of the model house ranged from a factor of two to a factor of ten greater in mass thickness. Thus, more material was placed in the direct path of above-ground radiation in the model, increasing the radiation scattered toward the basement, while the attenuation of the first floor remained the same in the model as in the full-scale house.

3. The density of the ground near the model basement wall was not scaled up as other materials (concrete blocks were substituted for soil with an accompanying density increase factor of only 1.5 instead of the 12 needed). For close-in source positions, considerable short-circuiting of gamma rays from source directly to detector would occur in the model, but not in the full-scale house. This is perhaps the most important reason.

## CHAPTER 5

### SUMMARY

The major portion of the effort and funds allocated for this project were devoted to the construction of an irradiation facility for the conduction of tests on model structures and the further verification of the modeling technique as a means of economically obtaining shielding data on real structures. The success of the project is best described in terms of the ease with which model radiation experiments may be carried out at the facility and accuracy obtained in modeling two previously tested full-scale structures. The major achievements of the program are:

1. The construction of a test facility for measurement of the shielding afforded by real structures through use of the modeling technique.
2. The ability of the test facility, as presently constructed, to allow several radiation exposures to be made in one day
3. Experimental verification of the modeling technique as a new and valuable concept in shielding analysis and experimentation
4. The generation of new experimental data on the protection factor offered by residential type structures.

APPENDIX A  
NORMALIZATION OF MODEL DATA

PRECAST CONCRETE HOUSE SOURCE RING NORMALIZATION

Full scale data<sup>1, 2</sup> for source ring experiments on the precast concrete house were presented in terms of dose rate for a source ring strength of 2 millicuries per foot of ring circumference ( $\frac{\text{mr/hr}}{2 \text{ mc/ft}}$ ). The model experiments for this building were performed on a 1/12-scale model of the structure and utilized a source ring also 1/12 the physical dimensions of the ring used for the full-scale experiments. For convenience in comparing the scale-model results with those of the full-scale building, it was necessary to normalize the model data to obtain values directly comparable to the full-scale results. The gamma-ray dose obtained for the model was therefore normalized to give results in terms of  $\frac{\text{mr/hr}}{2 \text{ mc/ft}}$  (full-scale). Readings of the dosimeters used in the model experiments in microamperes ( $\mu\text{a}$ ) were converted to  $\frac{\text{mr/hr}}{2 \text{ mc/in}}$  (model) which represents  $\frac{\text{mr/hr}}{2 \text{ mc/ft}}$  (comparable full-scale) as follows:

For reader values between 0 and 25  $\mu\text{a}$ :

$$\frac{\text{mr/hr}}{2 \text{ mc/in}} = \mu\text{a} \left( \frac{\text{mr}}{\mu\text{a}} \right) \left( \frac{1}{\text{time-hr}} \right) \left( \frac{2}{\frac{\text{source strength-mc}}{\text{ring circumference-in.}}} \right) \frac{1}{144}$$

$\downarrow$   
Conversion  
of  $\mu\text{a}$  to mr

$\downarrow$   
Conversion  
to per-hour

$\downarrow$   
Conversion of activity  
in ring to 2mc/in. basis

$\downarrow$   
Scale  
factor

From the calibration results (page 12) of the 2r dosimeters, the calibration factor for dosimeter readings between 0 and 25  $\mu\text{a}$  was 16 mr/ $\mu\text{a}$ . Between 25 and 100  $\mu\text{a}$ , however, the dose was 150 mr less than 21.4 mr/ $\mu\text{a}$ , because of the bend in the calibration curve at 25  $\mu\text{a}$ .

<sup>1</sup>J. A. Auxier, J. O. Buchanan, C. Eisenhauer, and H. E. Menker, "Experimental Evaluation of the Radiation Protection Afforded by Residential Structures against Distributed Sources," CEX-58.1, AEC, 19 Jan. (1959).

<sup>2</sup>C. Eisenhauer, "Analysis of Experiments on Light Residential Structures with Distributed Co<sup>60</sup> Sources," NBS No. 6539, 15 Oct. (1959).

The source ring strength of 2 mc/ft for the full-scale ring experiments gave the same total ring strength as 2 mc/in. did for a ring of 1/12 the physical dimensions. Thus, dose rate at comparable positions in the buildings will be  $(12)^2$  or 144 times greater than for the model experiments. The factor of 144 was based on the dose rate varying inversely as the square of the distance of the source from the detector and neglects minor factors, such as the difference in air absorption, air scattering, and ground scattering of the gamma rays between the full-scale and model arrangements. The error due to neglecting air absorption differences in the comparison of the direct-radiation dose rates for the model and full-scale experiments was calculated to be 5.4 and 9.2 per cent respectively for the 25.5- and 42.5-inch rings. This was usually within the accuracy of the experimental measurements.

The error due to the difference in build-up in the air caused by air and ground scattering of the gamma rays is best estimated by referring to the build-up experiments reported elsewhere.<sup>3</sup> The observed build-up factor, B, for a source-to-dosimeter distance of only 25.5 inches at a height of 1 foot was 1.24, while for a source-to-dosimeter distance of 25.5 feet, the build-up factor at the 3-foot level was 1.13. This would induce an error of approximately 9.7 per cent, if the build-up were the same at the 3-inch level as at the 1-foot level. Unfortunately, there is no further available data to substantiate build-up values at source-to-dosimeter distances less than 0.01 mean free paths in air and at dosimeter heights of 1 foot or less. For build-up comparisons for the 42.5-inch ring with the 42.5-foot, full-scale ring, the build-up factors are 1.20 and 1.17 respectively. Error in normalization for the 42.5-inch ring experiment from neglecting build-up is thus only 2.5 per cent. The data in footnote 3 indicate that the build-up contribution for the 25.5-inch ring experiments will be greater than for the 42.5-inch ring because of a rapid increase in build-up at small source-to-dosimeter distances and low dosimeter heights. Thus, normalized data as presented in this report should be in the order of 15 per cent higher than comparable full-scale data for the 25.5-inch ring experiments and 12 per cent for the 42.5-inch ring experiments.

<sup>3</sup>R. E. Rexroad and M. A. Schnoke, "Scattered Radiation and Free-Field Dose Rates from Distributed Cobalt-60 and Cesium-137 Sources," NDL, TR-2, September (1960).

## TWO-STORY HOUSE AREA SIMULATION

The experimental data obtained from area simulation of fallout radiation may be normalized to several convenient source densities. However, for convenience, the area data presented in this report have been normalized to a source strength of 0.024 curie per square meter. An infinite flat field of this cobalt-60 source density would provide a dose rate of one roentgen/hr at a height of 1 meter under standard atmospheric conditions (mean free path of 135 meters). Thus, normalization was accomplished as follows:

$$\begin{array}{ccccccc}
 \frac{\text{mr/hr}}{\downarrow} & = & \mu a \left( \frac{\text{mr}}{\mu a} \right) & \left( \frac{1}{\text{time - hr}} \right) & \left( \frac{0.024 \frac{\text{curie}}{\text{meter}^2}}{\frac{\text{source strength (curies)}}{\text{area of simulated field (meter}^2)}} \right) \\
 \text{Simulated from} & & \downarrow & \downarrow & \downarrow \\
 \text{a field of 0.024} & & \text{Conversion of} & \text{Total} & \text{Normalization for source} \\
 \text{curie/meter}^2 & & \mu a \text{ to mr} & \text{exposure} & \text{strength} \\
 & & & \text{time} & 
 \end{array}$$

APPENDIX B  
TRANSPARENT-BUILDING CALCULATIONS

PRESENT CONCRETE HOUSE WITH SOURCE RINGS

Dose rate was calculated for dosimeter locations within a transparent version of the precast concrete house. In this case, the dosimeter positions remain the same as during the source ring experiments on the building, but the mass of the building is assumed to be removed so that there is no absorption and scattering of gamma rays by the building structure. For these calculations, as for the comparison of full-scale and model data, both air absorption and air build-up were small enough factors to be omitted. Transparent-house dose rate calculations were made to obtain curves of dose rate versus distance (Figures B-1 and B-2) from the center of both the 25.5- and 42.5-foot source ring at heights of 1, 3, 5, and 7 feet. From these curves the dose rate at any dosimeter location could be rapidly determined. Transparent-building dose rate was calculated from the following equation:<sup>1</sup>

$$\frac{mr}{hr} = \frac{1000 q \Gamma}{[(a^2 + b^2 + h^2)^2 - 4a^2 b^2]^{1/2}} \quad (1-B)$$

where

	<u>Metric Units</u>	<u>English Units</u>
a =	Source ring radius (cm)	(ft)
b =	Distance from center of ring (cm)	(ft)
h =	Height above ring plane (cm)	(ft)
q =	Total millicuries of Co-60	---
$\Gamma$ =	$13.5 \text{ cm}^2 - r/\text{mc-hr}$	$0.0145 \text{ ft}^2 - \frac{r}{\text{mc-hr}}$

<sup>1</sup>G. J. Hine, and G. L. Brownell, "Radiation Dosimetry," Academic Press Inc. (1956), p. 762.



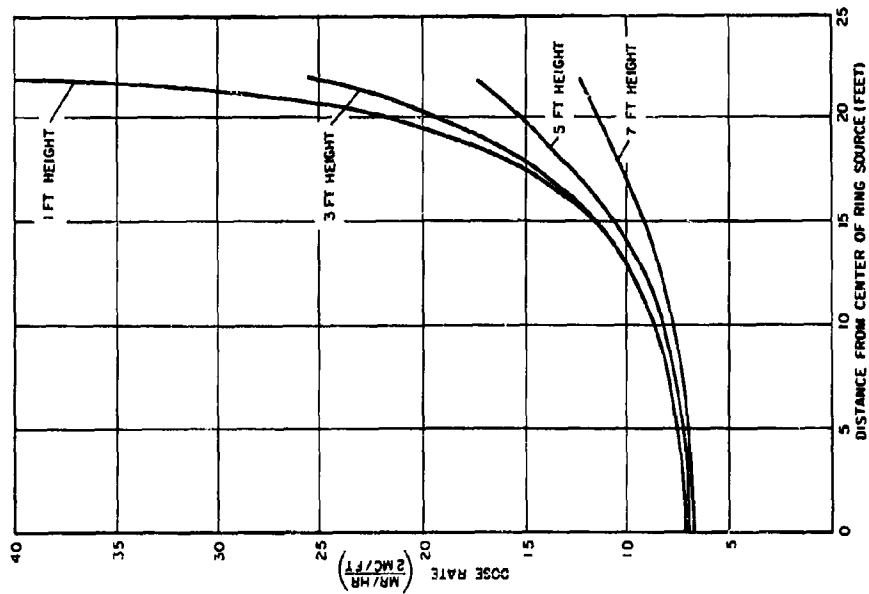


Figure B-1. Dose Rate for Transparent House in Center of 25.5 Foot-Radius Source Ring

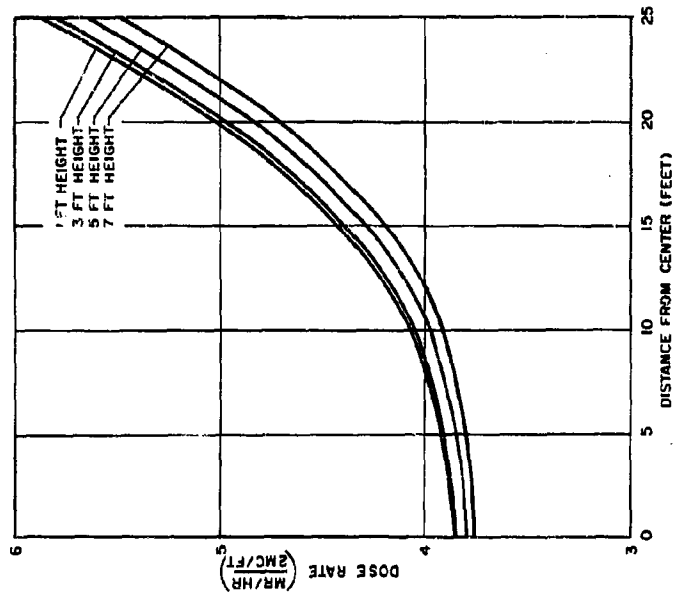


Figure B-2. Dose Rate for Transparent House in Center of 42.5 Foot-Radius Source Ring

## TWO-STORY MODEL BUILDING WITH AREA SPREAD

Dose rates within a phantom version of the two-story model building located at the center of the experimental area spread were calculated from equations presented in Appendix A of footnote 2. The following equations give approximate dose rates at locations above a cleared circle:

$$R_d \cong 2\pi\sigma q E_1 (\mu y) \quad (2-B)$$

$$R_s \cong 2\pi\sigma q k e^{-\mu y} \quad (3-B)$$

where

$R_d$  = Direct radiation (r/hr)

$R_s$  = Scattered radiation (r/hr)

$\sigma$  = Density of radiation field (curies/meter<sup>2</sup>)

$q$  = 1.35 r/hr per curie at 1 meter (cobalt-60)

$k$  = 0.55 (cobalt-60)

$\mu$  = Total linear absorption coefficient ( $7.41 \times 10^{-3}$ /meters)  
for cobalt-60 in air

$y$  =  $\left[ (a^2 + h^2 + x^2)^2 - 4x^2 a^2 \right]^{1/4}$

$a$  = Radius of cleared area (meters)

$h$  = Detector height above contaminated plane (meters)

$x$  = Horizontal distance of detector from center (meters).

Dose contributions from the actual area spread (finite field) were determined by evaluating these equations at the inner and outer boundaries of the area spread and determining their difference. This approximate solution gives exact values at all positions directly above or on the center of the cleared area, while values offset from the center will be somewhat low but appropriate for this particular model calculation. Curves of calculated dose rate versus dosimeter height at the center,

<sup>2</sup>Eric T. Clarke, John F. Batter, Jr., and Arthur L. Kaplan, "Measurement of Attenuation in Existing Structures of Radiation from Simulated Fallout," Technical Operations, Inc., Report TO-B 59-4, 27 April (1959).

at 10-1/4 inches from the center, and at the inner radius of the area spread are given in Figure B-3. Greater accuracy may be had, if the refined methods of calculation, as presented in Appendix C of this report, are used.

Calculated dose rates in a phantom model basement were determined by multiplying the dose rates of similar above-ground detector positions by reduction factors determined from the following equations and procedures:<sup>3</sup>

$$I/I_0 = e^{-3.2(1-\omega)} \quad \text{for } \omega > 0.3 \quad (4-B)$$

$$I/I_0 = \frac{\omega}{3} \quad \text{for } \omega < 0.3 \quad (5-B)$$

where

I = Intensity at basement position

I<sub>0</sub> = Reference intensity at same position above ground level

ω = Solid angle fraction.

Intensities and solid angles for a given point within the basement were obtained by dividing the basement area into four rectangles meeting at the desired point, calculating the solid angle fraction using the depth and four times the area of each rectangle, and obtaining the intensity contributions together and dividing by four.

---

<sup>3</sup>Clarke, Batter and Kaplan, op. cit., p. 57.

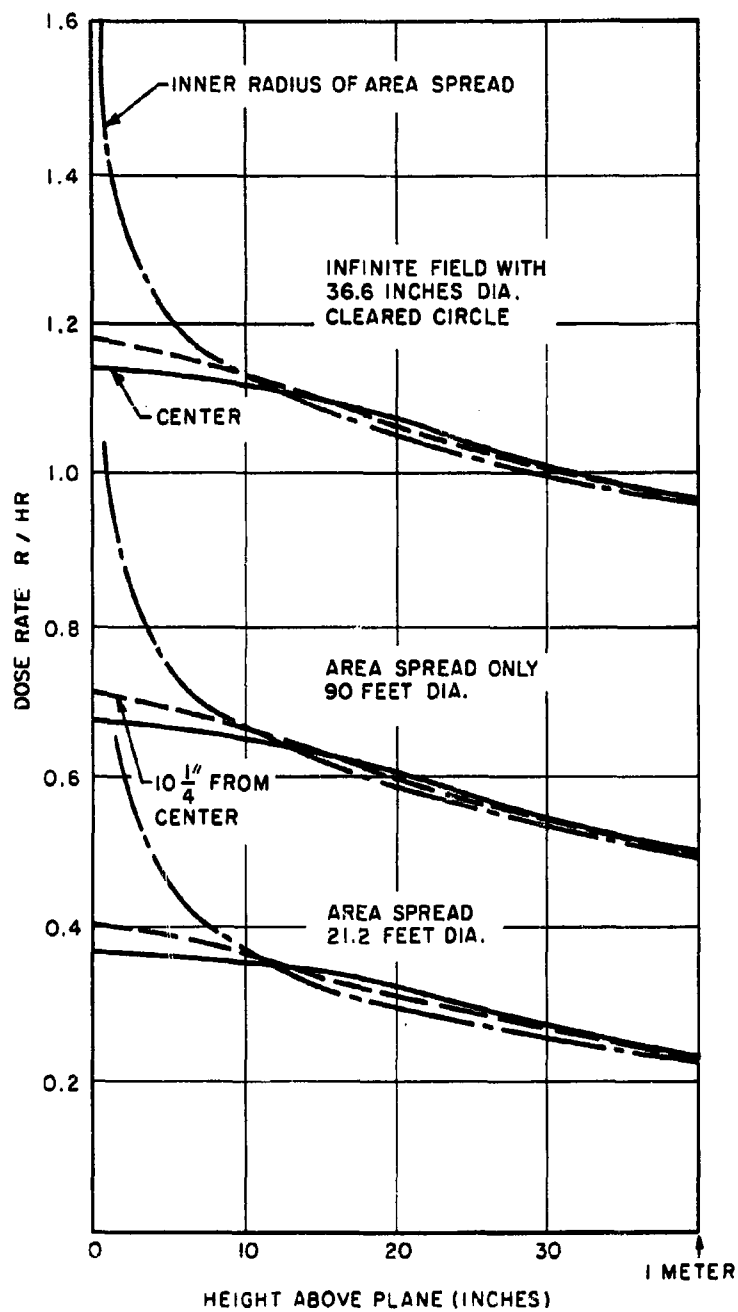


Figure B-3. Dose Rate Versus Dosimeter Height for Transparent Model House in Center of Annular Source Areas

## APPENDIX C

### DOSE RATES FROM ANNULAR SOURCE FIELDS

The problem of calculating dose rates inside or outside a transparent building is considered more fully below.

The refinements which are introduced result from appraising the validity of equations used in Appendix B for the different positions at which dose rates are to be calculated. These more refined calculations have not been done for comparison with the experimental work in this report, largely because the simpler calculations already presented form an adequate basis for judging data of the accuracy obtained. However, the presentation below provides a useful guide to the accuracy of the simpler calculations as well as a method for improving their accuracy when necessary.

#### VALIDITY OF APPROXIMATE FORMULATION USING A MEAN SOURCE-TO-DETECTOR DISTANCE

For a plane annular field of radiation source material, it is often necessary to calculate the dose rate at a detector somewhere in the vicinity of the center where no source material exists. The source material may be distributed outward over a finite or an infinite radial distance. A complete solution to the problem will provide the dose rate at every point in a cylindrical space which includes the cleared central area and all points above it. While it is possible to write a general solution, its evaluation usually requires numerical integration or use of approximations. The exceptions are for those points on the axis (at zero radius) at any height. We shall examine the validity of approximations which may be used so that sufficiently accurate dose rates for points off the axis may be calculated by means short of numerical integration.

A practical example of the conditions of the problem is a uniform distribution of fallout material over the plane earth surrounding a deep circular lake. To find the dose rate on and above the lake, we start by treating only an elemental ring of source material while assuming: 1) no source decay, 2) inverse square law behavior

between source material and detector, and 3) absorption by the medium through which the radiation passes. The dose rate due to direct radiation,  $dR_d$  (no contribution due to scattering) received by a point detector from one annular ring of radius  $r$  and elemental width  $dr$  is:

$$dR_d(h, x, r) = 2\sigma q r dr \int_0^\pi \frac{\exp - \mu \left[ r^2 + x^2 + h^2 - 2xr \cos \Theta \right]^{1/2}}{\left[ r^2 + x^2 + h^2 - 2xr \cos \Theta \right]} d\Theta \quad (1-C)$$

where

- $\sigma$  = Uniform source surface density in curies per unit area
- $q$  = Conversion factor to dose rate for the particular source material used (e. g.,  $q = 1.35$  roentgens per hour for one curie of Co-60 at 1 meter from the detector)
- $x$  = Horizontal distance of the detector from the center of the ring
- $h$  = Height of detector above the plane
- $\mu$  = Total linear absorption coefficient of the medium.

Equation (1-C) may be approximated by a simpler form which substitutes an effective mean distance from source to detector:

$$y = \left[ (r^2 + x^2 + h^2)^2 - 4x^2 r^2 \right]^{1/4} \quad (2-C)$$

for the actual distance which is:

$$\left[ r^2 + x^2 + h^2 - 2xr \cos \Theta \right]^{1/2} \quad (3-C)$$

Then (1-C) becomes:

$$dR_d \cong 2\pi \sigma q r dr \frac{\exp - (\mu y)}{y^2} \quad (4-C)$$

within the accuracy of the substitution just made.<sup>1</sup> Before extending (4-C) to give the dose rate from an annular source field wider than  $dr$ , we must consider the

<sup>1</sup>The quantity,  $y$ , is the geometric mean distance from the detector to the nearest and farthest points on the elemental source ring. For the simpler cases mentioned, note that  $y = (r^2 + h^2)^{1/2}$  when  $x = 0$ . Then equation (2-C) is exact.

validity of the use of  $y$ ; that is, we must investigate the domain in which approximation (4-C) gives an adequate description of the dose rate of equation (1-C). A comparison can be made between the following relations which are functionally equivalent to (1-C) and (4-C) respectively:

$$I(\eta) = \frac{1}{P^2} \int_0^\pi \frac{e^{-\mu P [1 - \eta \cos \Theta]}^{1/2}}{[1 - \eta \cos \Theta]} d\Theta \quad (5-C)$$

and

$$A(\eta) = \frac{\pi e^{-\mu P [1 - \eta^2]^{1/4}}}{P^2 [1 - \eta^2]^{1/4}} \quad (6-C)$$

where:

$$P = [r^2 + x^2 + h^2]^{1/2} \quad (7-C)$$

$$\eta = 2rx/P^2 \quad (8-C)$$

From (8-C) it can be seen that variations in  $x$  can be investigated through  $\eta$  as long as  $r$  and  $P$  are held constant. For variable  $\eta$  and fixed  $P$ , a comparison of (5-C) and (6-C) is facilitated by Taylor expansions about  $\eta = 0$ :

$$\left. \begin{aligned} \frac{P^2 e^{\mu P}}{\pi} I(\eta) &\approx \left[ 1 + \frac{1}{2} \left\{ 1 + \frac{5(\mu P)}{8} + \frac{(\mu P)^2}{8} \right\} \eta^2 \right. \\ &\quad \left. + \frac{3}{8} \left\{ 1 + \frac{279}{384} (\mu P) + \frac{87}{384} (\mu P)^2 + \frac{7}{192} (\mu P)^3 + \frac{(\mu P)^4}{384} \right\} \eta^4 \right] \end{aligned} \right\} \quad (9-C)$$

$$\frac{P^2 e^{\mu P}}{\pi} A(\eta) \approx \left[ 1 + \frac{1}{2} \left\{ 1 + \frac{1}{2} (\mu P) \right\} \eta^2 + \frac{17}{48} \left\{ 1 + \frac{9}{34} (\mu P) + \frac{2}{17} (\mu P)^2 \right\} \eta^4 \right] \quad (10-C)$$

It is apparent that for  $\eta > 0$ ,  $A(\eta) < I(\eta)$ . That is, while expression (4-C) can never exceed the true dose, it should be a valid approximation for small  $\eta$  (hence, large  $P$  and/or small  $x/r$ ).

This assertion can be investigated by utilizing a typical set of parameter values encountered in practice. For  $r = 100$  feet,  $x = 25$  feet,  $h = 25$  feet,  $P = 106.1$  feet and  $\mu^{-1} = \lambda = 448$  feet (Co-60 radiation in air):

$$\frac{P^2 e^{\mu P}}{\pi} I(\eta) \approx 1 + 0.5775 \eta^2 + 0.4445 \eta^4 + \dots \quad (11-C)$$

$$\frac{P^2 e^{\mu P}}{\pi} A(\eta) \cong 1 + 0.5592 \eta^2 + 0.3787 \eta^4 + \dots \quad (12-C)$$

Table I-C compares (11-C) and (12-C) for values of  $\eta \leq 0.5$ . As would be expected, the difference between the two functions increases with increasing  $\eta$ , reaching a difference of slightly less than 1 per cent for the value  $\eta = 0.5$ . It is significant to note that even for  $\eta = 0.5$ , the sixth order term in (11-C) (the expansion representing the precise dose rate of (1-C)) is roughly 1 per cent of the fourth order term, or 0.002 per cent of the zero order term. Consequently, Equation (11-C) represents the true dose rate quite closely for  $\eta \leq 0.5$ . It follows that approximation (4-C) is valid to within 1 per cent in this domain. (For the values assumed above, one actually finds  $\eta = 0.46$ .)

To further estimate the effect of  $r$ , the ring radius, in the above calculations, the functions  $I(\eta)$  and  $A(\eta)$  are again obtained from Equations (9-C) and (10-C) for the same detector position,  $x = 25$  feet and  $h = 25$  feet, but a radius corresponding to  $P = \mu^{-1} = 448$  feet.

For these conditions:

$$\frac{P^2 e^{\mu P}}{\pi} I(\eta) = 1 + 0.875 \eta^2 + 0.747 \eta^4 \quad (13-C)$$

$$\frac{P^2 e^{\mu P}}{\pi} A(\eta) = 1 + 0.75 \eta^2 + 0.790 \eta^4 \quad (14-C)$$

TABLE I-C

COMPARISON OF TAYLOR EXPANSIONS OF TRUE DOSE FUNCTION,  $I(\eta)$ , WITH APPROXIMATE DOSE FUNCTION,  $A(\eta)$ , FOR  $P = 106.07$  FEET,  $\mu = 448$  FEET

$\eta$	$\frac{P^2 e^{\mu P}}{\pi} A(\eta)$	$\frac{P^2 e^{\mu P}}{\pi} I(\eta)$
0.1	1.00563	1.00582
0.2	1.02300	1.02380
0.3	1.05340	1.0555
0.4	1.09920	1.10378
0.5	1.1635	1.17220



Here, although the expansion coefficients have increased slightly, the value of  $\eta$  is now decreased from  $\eta = 0.46$  to  $\eta = 0.11$ . It is again evident that  $I(\eta)$  of Equation (13-C) will be quite close to the true dose rate of equation (1-C) for values of  $\eta$  in the region  $\eta \leq 0.5$ . Consequently, approximation (4-C) goes from roughly 1 per cent error at  $P = 106.07$  feet to roughly a 0.1 per cent error at  $P = 448$  feet.

Thus, for most conditions encountered in practice, expression (4-C) will be valid in the region  $\eta \leq 0.5$ . This corresponds to:

$$4 \, r x \leq r^2 + x^2 + h^2 \quad (15-C)$$

or

$$4 \leq \left(\frac{r}{x}\right) + \left(\frac{x}{r}\right) + \frac{h^2}{rx} \quad (16-C)$$

The latter inequality is satisfied (independent of  $h$ ) for all  $x$  in the region:

$$x \leq r/4 \quad (17-C)$$

Thus, Equation (4-C) is a valid approximation of dose rate for all detector positions of eccentricity not exceeding one quarter of the radius of the annular source ring. Moreover, if condition (17-C) is satisfied for the inner boundary of an annular source field of finite width, expression (4-C) can be integrated over  $r$  to obtain the total dose from this (finite or infinite) field.

#### EVALUATION OF DOSE RATES FOR AN INFINITE FIELD FROM THE APPROXIMATION FORMULATION

The total dose rate from an annular field extending to infinity can be divided into contributions,  $R_d$  and  $R_s$ , due to direct and scattered radiations respectively, as follows:<sup>2</sup>

$$R_d \approx 2 \pi \sigma q I_d \quad (18-C)$$

$$R_s \approx 2 \pi \sigma q k I_s \quad (19-C)$$

<sup>2</sup>E. T. Clarke, J. F. Batter and A. L. Kaplan, "Measurement of Attenuation in Existing Structures of Radiation from Simulated Fallout," Technical Operations, Inc., Report No. TO-B 59-4, Appendix E, 27 April 1959.

in which:

$$I_d = \int_{y_1}^{\infty} \frac{y e^{-\mu y} dy}{(y^4 - 4h^2 x^2)^{1/2}} \quad (20-C)$$

$$I_s = \mu \int_{y_1}^{\infty} \frac{y^2 e^{-\mu y} dy}{(y^4 - 4h^2 x^2)^{1/2}} \quad (21-C)$$

where  $y_1$  is that value of  $y$  corresponding to  $r$  at the inner edge of the annulus. Expressions (18-C), (19-C), (20-C), and (21-C) were obtained by multiplying (4-C) by the "build-up" factor  $B = 1 + k\mu y$  before integration. The constant  $k$  is dimensionless and depends on the energy of the source and on the surrounding medium. Both  $I_d$  and  $I_s$  are dimensionless.

The integrals (18-C), (19-C) are difficult to evaluate unless  $y^4 \gg 4h^2 x^2$  for all  $y$ . At the same time, their formulation in terms of  $y$  is valid (for all  $h$ ) for only a restricted range of  $x$ . We now consider whether these two conditions occur together. The following relation is equivalent to (2-C) which defines  $y$ :

$$y^4 - 4h^2 x^2 = (r^2 + h^2 - x^2)^2 \quad (22-C)$$

The validity condition (17-C) may be applied to (22-C). This is conveniently done by taking the ratio  $4h^2 x^2 / (r^2 + h^2 - x^2)^2$ . The result is:

$$4h^2 x^2 < y_1^4 \leq y^4 \quad (23-C)$$

That is, (23-C) holds over the entire range of  $x$  through which (18-C), (19-C) represent sufficiently accurate dose rates. Now the integrals of (20-C) (21-C) may be approximated by use of a finite number of terms resulting from the binomial expansion of the denominator:

$$(y^4 - 4h^2 x^2)^{-1/2} = y^{-2} \left[ 1 + \frac{2h^2 x^2}{y^4} + 6 \left( \frac{h^2 x^2}{y^4} \right)^2 + \dots \right] \quad (24-C)$$

Consequently, the integrals (20-C), (21-C) become:

$$I_d = \int_{y_1}^{\infty} \frac{e^{-\mu y}}{y} \left[ 1 + 2 \left( \frac{h^2 x^2}{y^4} \right) + 6 \left( \frac{h^2 x^2}{y^4} \right)^2 + \dots \right] dy \quad (25-C)$$

$$I_s = \mu \int_{y_1}^{\infty} e^{-\mu y} \left[ 1 + 2 \left( \frac{h^2 x^2}{y^4} \right) + 6 \left( \frac{h^2 x^2}{y^4} \right)^2 + \dots \right] dy \quad (26-C)$$

The simpler cases mentioned earlier result from terminating the series after the first term. These are the zero order expressions (13)<sup>3</sup> which are independent of the parameters of interest,  $h$ ,  $x$ , and  $y_1$ . For this dependence, higher order terms may be found with the following identity:

For  $n$ , an integer greater than unity,

$$\int_a^{\infty} y^{-n} e^{-\mu y} dy = e^{-\mu a} \left\{ \sum_{P=1}^{P=(n-1)} \left[ \frac{(-1)^P a^{-(n+P)} \mu^{P-1}}{(-n+1)(-n+2) \dots (-n+P)} \right] + \frac{\mu^{n-1}}{(-n+1)(-n+2) \dots (-1)} E_1(\mu a) \right\} \quad (27-C)$$

where  $E_1(\mu a)$  denotes the exponential integral.

For example, when (27-C) is applied to (25-C), (26-C) first order, we have:

$$I_d = \left[ 1 + \frac{\alpha \beta^4}{12} \right] E_1(\beta) + \frac{\alpha}{2} e^{-\beta} \left[ 1 + \frac{\beta}{3} + \frac{\beta^2}{6} + \frac{\beta^3}{6} \right] \quad (28-C)$$

$$I_s = e^{-\beta} \left[ 1 + \frac{2}{3} \alpha \beta + \frac{\alpha \beta^2}{3} + \frac{\alpha \beta^3}{3} \right] - \frac{\alpha \beta^4}{3} E_1(\beta) \quad (29-C)$$

where

$$\alpha = h^2 x_1^2 / y_1^4 \text{ and } \beta = \mu y_1.$$

If  $\beta \ll 1$ , only linear and bi-linear terms in  $\alpha$  and  $\beta$ , respectively, need be retained. (For Co-60,  $\beta \ll 1$  implies that  $y_1 \ll 450$  feet.) Under such conditions:

$$I_d \cong E_1(\beta) + \frac{\alpha}{2} e^{-\beta} \left[ 1 + \frac{\beta}{3} \right] \quad (30-C)$$

$$I_s \cong e^{-\beta} \left[ 1 + \frac{2}{3} \alpha \beta \right] \quad (31-C)$$

<sup>3</sup>Clarke, Batter, and Kaplan, op. cit.

Utilizing the above equations, the dose from any annulus satisfying the conditions  $\alpha \ll 1$ ,  $\beta \ll 1$  can be calculated and a direct comparison of this first order result made with the zero order result.

Consider, for example, the Long Island barracks experiment (mentioned in footnote 3) described by  $a = 100$  feet,  $b = 125$  feet and a detector position  $h = 24$  feet,  $x = 75$  feet.

For the inner boundary ( $a = 100$  feet):

$$\begin{aligned} \alpha &\cong 0.083 & \beta &\cong 0.174 \\ I_d &\cong 1.338 + [0.036] \\ I_s &\cong 0.84 + [0.008] \end{aligned} \quad (32-C)$$

At the outer boundary ( $a = 125$  feet)

$$\begin{aligned} \alpha &\cong 0.011 & \beta &\cong 0.23 \\ I_d &\cong 1.110 + [0.0046] \\ I_s &\cong 0.794 + [0.0013] \end{aligned} \quad (33-C)$$

where the bracketed terms represent the first order contribution. Utilizing the value of  $k = 0.55$ , we find that the zero order calculation for dose under these conditions is approximately 14 per cent lower than the first order calculation.

In contrast to these results, we can calculate the dose received for the case described above by direct numerical integration. As reported in footnote 2, such a calculation demonstrates that the zero order calculation is 12 per cent too low. Consequently, the first order calculation based on equations (30-C), (31-C) yields a dose which is only 2 per cent higher than that obtained by direct numerical integration.